Coordination Chemistry Reviews 495 (2023) 215342

Contents lists available at ScienceDirect

Coordination Chemistry Reviews

journal homepage: www.elsevier.com/locate/ccr

Evolution of covalent organic frameworks: From design to real-world applications

Jesús Á. Martín-Illán [a], David Rodríguez-San-Miguel [a,b], Félix Zamora [a,b,c,*]

[a] Universidad Autónoma de Madrid, Facultad de Ciencias, Departamento de Inorgánica, Madrid 28049, Spain
[b] Institute for Advanced Research in Chemical Sciences (IAdChem), Universidad Autónoma de Madrid, 28049 Madrid, Spain
[c] Condensed Matter Physics Center (IFIMAC), Facultad de Ciencias, Universidad Autónoma de Madrid, Madrid 28048, Spain

ARTICLE INFO

Keywords:
Covalent Organic Frameworks
COFs preparation
COFs procesability
COFs uses

ABSTRACT

Covalent Organic Frameworks are highly versatile porous materials that have attracted much attention over the last few years. This review summarizes the timeline of its development, highlighting the shifts in the targets deemed necessary to use them in real-world applications. We have collected aspects concerning COF formation and the strategies developed to gain chemical stability by using different linkages between the initial building blocks and modulating the structural characteristics of COFs. Importantly, we have also included elements concerning material processability that has been incorporated in the research field of COFs but are essential to solving many different applications of COFs. Finally, we included a summary section providing headlines of this research field to get closer to real applications.

1. Introduction

Any solid with a void area (or spaces) that are not occupied by the main atomic framework and provides the solid with certain unique qualities is said to have pores. Since the advent of contemporary frameworks, there has been a notable increase in scientific interest. But it is essential to recognize that humans have used porous materials for much longer than we might immediately believe. Examples of this widely used substance include wood, charcoal, and pottery. For instance, porous materials were employed medicinally by the ancient Egyptians. Reports from the Ebers papyrus from 1500 BCE mention therapeutic techniques using charcoal to treat dyspepsia [1].

Due to its adsorptive qualities, charcoal was still used in experimental gastrointestinal disorders treatments in the early modern age. However, it was not until Scheele, Priestley, and Fontana studied the gas adsorption within charcoal in 18th-century Europe that we began to think about the scientific ideas of adsorption employing porous materials [2]. Zeolites, another outstanding milestone porous substance, gained fame in the scientific world in the same period. Cronstedt discovered natural zeolites, aluminosilicate mineral compounds with finely organized pores, in 1756 [3]. Over a century after, in 1862, Sainte-Claire-Deville produced the first artificial zeolites, lévyne or levynite [4]. However, the interest in these niche materials had been limited until, in the 1940s, Barrer established the field of modern synthetic zeolite [5]. Subsequently, Kistler developed more ordered porous materials, such as silica aerogel, produced in 1931. These mesoporous materials exceeded the pore size limits of zeolites (~2 nm) while taking advantage of the robust chemical benefits of silica [6].

Porous polymer networks (PPNs), a porous polymeric structure based on non-intrinsically systems, first appeared in the late 1940s, but it was not until the 21st century that it was thoroughly researched. Prof. Robson, by the end of the '80s [7], and Prof. Kitagawa demonstrated that coordination polymers and complexes might be remarkably crystalline in the 1990s [8].

In response to the development of porous coordination materials, Prof. Yaghi and col. created planned, stable, and permanently porous metal–organic frameworks in the late 1990s (MOFs) [9]. Due to the widespread interest in MOFs, research on novel materials with comparable properties, including highly ordered porosity and design through the self-correction of non-covalent interactions, has been conducted. Makoto Fujita thus discovered porous coordination cages (PCCs) in 1990 [10]. Later, the concept of PCCs mixed with intrinsically porous polymers (PIMs) [11] gave rise to porous organic cages [12]. The challenge of control over the design of extended organic solids based on covalent bonds meant that they remained largely undeveloped throughout the 20th century.

* Corresponding authors.
E-mail address: felix.zamora@uam.es (F. Zamora).

https://doi.org/10.1016/j.ccr.2023.215342
Received 27 February 2023; Received in revised form 19 May 2023; Accepted 5 July 2023
Available online 8 August 2023
0010-8545/© 2023 The Authors. Published by Elsevier B.V. This is an open access article under the CC BY license (http://creativecommons.org/licenses/by/4.0/).

Thus, a reticulation process must be carried out under synthetic conditions that maintain the molecule's stability while allowing microscopic reversibility to afford ordered, crystalline products [13]. The challenge was addressed in the discovery of two-dimensional (2D) and three-dimensional (3D) covalent organic frameworks (COFs) [14], in which extended networks are made by stitching organic molecules together through strong covalent bonds in a process termed reticular synthesis. The well-defined crystalline porous structures and tailored design offered COFs various applications, such as gas storage, ionic conductors, energy storage and production, sensing, adsorption, optoelectronic, and catalysis [15].

In this review, we aim to show the temporal evolution of the research trends in COFs, showcasing the most significant advances in each period. We will start discussing the search for new network topologies and linkages initiated after the first report in 2005 until we reach the current state, in which the main focus is set on improving the methods for incorporating them in working devices.

2. Covalent organic frameworks

Covalent organic frameworks, or COFs for short, are well-defined primary and high-order structures that can incorporate organic units. Prof. Yaghi and col. originally reported on synthesizing such an organic solid porous crystalline polymer in 2005 [16]. This new material's discovery broadens the application of reticular synthesis beyond its coordination equivalent, metal–organic frameworks, to its solely organic constituents [14]. Since that time, COF research has rapidly grown to become a multidisciplinary subject with a wide range of applications.

2.1. General aspects of COFs

COFs are tailored and designable materials. The properties can be modified by selecting between the different monomers or building blocks and types of bonds such as topology, stability, functional moieties, etc. Thus, structural design can be associated with the Lego® game, in which building blocks, as shown in Fig. 1, can be simplified as geometrical pieces that can be linked through the vertices creating a periodic and ordered network. Although some molecules or bonds are restricted to certain symmetries, the wide variety of available building blocks has led to the development of various COFs structures. The subsequent discussion deals with these aspects that must be decided to design a COF [17].

2.2. Topology

Conceptually, the critical element in the layout of new COFs is the topological design, which will significantly influence the primary intrinsic properties of COFs, i.e., crystallinity and porosity. As monomers determine the framework structure, COFs are fully predesignated and synthetically controllable polymers. COFs utilize step-growth polymerization for chain propagation in a 2D or 3D manner (Fig. 2). The polymerization process involves the integration of both covalent bonds and non-covalent interactions in shaping well-defined yet extended crystalline structures. In 2D-COFs, the network is restricted to propagating covalent bonds in a plane, forming layers. As expected, non-covalent interaction, aromatics, π-staking, hydrogen bonds, and van der Waal's forces prevent these layers from remaining isolated, tending to aggregate, and forming layered material. 3D topologies allow the extension of covalent bonds in all directions. The material is isotropic, generating lattice structures supported solely by the same type of interaction in every direction. However, since the first synthesis reported of 3D-COFs in 2007 [18], only a handful of new 3D-COF structures have been reported. With the limited number of topologies and building blocks, most reported network examples rely on tetrahedral nodes such as ctn, bor, dia, or pts, which is related to the difficulty of obtaining organic monomers with another type of vertices as, for example, octahedra [19].

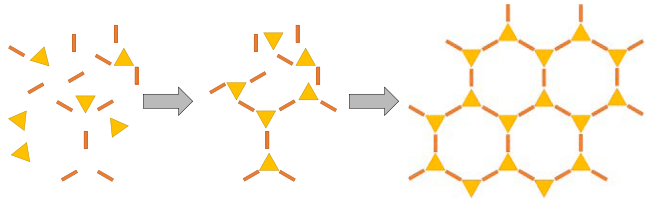

Fig. 1. Diagram showing how two building-blocks with the right geometry and functional groups can be combined to make a 2D hexagonal COF. Adapted from reference 88 with permission of the copyright holders.

2.3. Linkages

Since the type of bond is related to essential properties, the reaction between building blocks is one of the most important aspects of COFs modeling following the topological design. Therefore, the linkage formation must be reversible to produce extended crystalline solids under the reaction conditions. Then, the issue of crystallization must be resolved for each new bond, and synthetic conditions for crystalline framework materials must be developed [20]. Additionally, the reaction rates must be quick enough to allow for adequate self-correction of flaws [21]. Even precise adjustments to variables such as temperature, reaction time, concentration, and catalysis can substantially affect the crystallinity and porosity of the end product.

Additionally, as predicted theoretically, rings with diverse shapes were formed due to a tiny variation in bond angles permitted by a specific amount of strain on the stiff molecules [22]. Even more problematic is the bond out of the plane formed in laminar networks, which leads to interlayer cross-linking bonds, disturbing the structure. Nevertheless, covalent bonds' reversibility lets break incorrectly-formed bonds and links into an appropriate and thermodynamically stable network.

Several linkages have been developed over the years, summarized in Fig. 3, and will be discussed in the following paragraphs. The first COFs reported by Yaghi [14] and Lavigne [23] used the self-condensation of boronic acids to produce boroxine and boronate ester from condensations of boronic acids and catechols. Since then, COF, which contains boron, has become one of the most popular varieties. These connections offered exceptional thermal stability in general. The first alternative example after boron-containing COFs was triazine-based frameworks (CTFs), described by Kuhn and associates in 2008 [24]. This C-N bond-based structure, which is more stable than boronic ester structures, is created by cyclotrimerizing 1,4-dicyanobenzene at 400 °C in molten $ZnCl_2$. However, their appeal has been constrained by difficult synthesis conditions, which include an ionothermal procedure [25]. A well-intended but challenging issue was the further development of CTFs, particularly syntheses with improved crystallinity and functional group tolerance.

When Prof. Yaghi and col. created the first COF with imine bonds in 2009, it represented a significant advancement in the field of COFs [26]. Condensation between an aldehyde and a primary amine produces this imine-based COF. Additionally, imine condensation is easily accessible for synthesizing COFs due to the wide range of aldehyde and primary amine monomers.

The use of these linkages can be combined in the same network to increase the variety of possible structures and designs. Early examples in 2015 used a linear building block with both a boronic acid and an aldehyde that reacted with appropriate trigonal linkers forming a mixed boronate ester-imine COF [27]. Another common way to generate multicomponent COFs is to use mixtures of linear building blocks with different lengths, resulting in lower symmetry networks [28] or the combination of the same COF of pore sizes not achievable for a network with just two components [29]. More recently, examples have appeared using mixed trigonal building blocks, thus generating a honeycomb

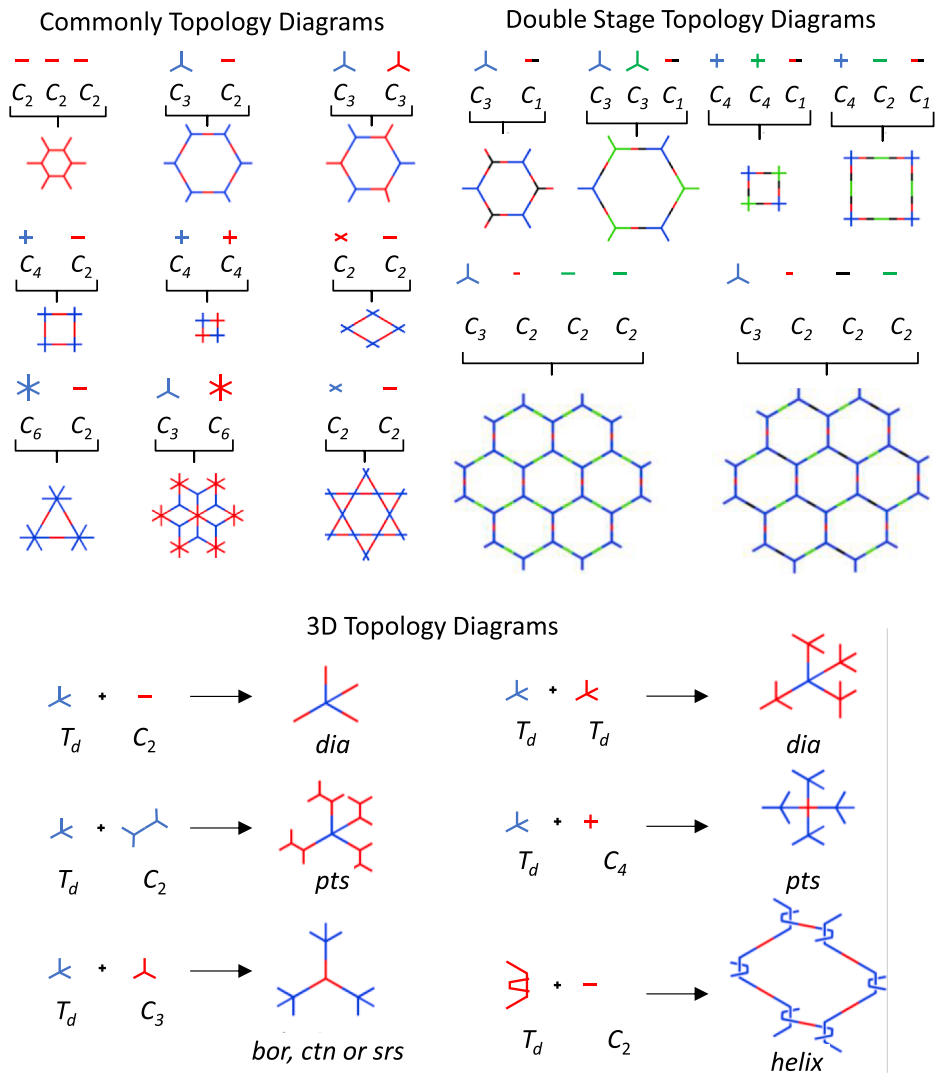

Fig. 2. Topology diagrams for designing 2D COFs and 3D COFs to create different skeletons and pores. Adapted from reference 14 with permission of the copyright holders.

network where the corners alternate between two molecules with different functionalities [30].

In recent years, the research of novel types of reversible covalent bonding has been extensively studied in COFs, and their effects on the materials' structural properties have been investigated in depth. For instance, the excellent reversibility of olefin (C═C) linkages means that COFs containing this type of linkage can undergo reversible structural changes under specific conditions, benefiting various applications, such as sensing and drug delivery [31]. Moreover, their high stability and strong π-conjugation can impart electronic properties to the network. For example, olefin-linked COFs can exhibit semiconduction behavior and efficient photocatalytic activity [32]. Furthermore, the reversibility of C═C linkages in COFs has been shown to be higher than that of 1,4-dioxin and viologen linkages. However, the 1,4-dioxin and viologen linkages are relatively less reversible, resulting in increased stability of the COFs. 1,4-dioxin-linked COFs are a type of covalent organic framework (COF) that is formed by the self-condensation of a catechol or a substituted catechol with an aldehyde or a substituted aldehyde [33]. Instead, viologen-linked COFs are constructed *via* reversible imine linkages between viologen and dialdehyde building blocks [34]. Both of them have attracted significant attention in recent years due to their potential applications in electrochromic devices, gas storage, and separation membranes [15]. Viologen linkages offer an advantage in their tunable redox properties, which can be utilized for redox-triggered switching of optical and electronic properties of the resulting COFs [35]. Both viologen and 1,4-dioxin-linked COFs, can be advantageous in applications where durability is critical, such as in catalysis and gas separation.

Nevertheless, the crystallinity-stability-functionalization trichotomy is a bottleneck to developing novel COFs. The linkage reversibility is inversely related to chemical stability. The more reversible the linkage is, the more vulnerable it is to adopt the minimum thermodynamic structure (Fig. 4). For example, boroxine-based COFs can be easily achieved but are susceptible to hydrolyzing; the empty orbital of the boron atoms makes them prone to hydrolysis (Fig. 5a), hindering their use in real applications that expose them to ambient conditions. In turn, imine-based COFs are more challenging to synthesize but are more robust; this type of linkage has become one of the most widely used for the obtention of COFs [21,36]. However, their thermal stability is poorer than that of their boronate-ester-linked counterparts, and their chemical stability is not acceptable for severely acidic circumstances.

The investigation of alternative linkage based on C-N bonds was stimulated by the tolerance range of reaction conditions from ambient temperature to solvothermal synthesis, resulting in the invention of hydrazine [37], imide [38], azine [39], amide [40] and squaraine-linked [41].

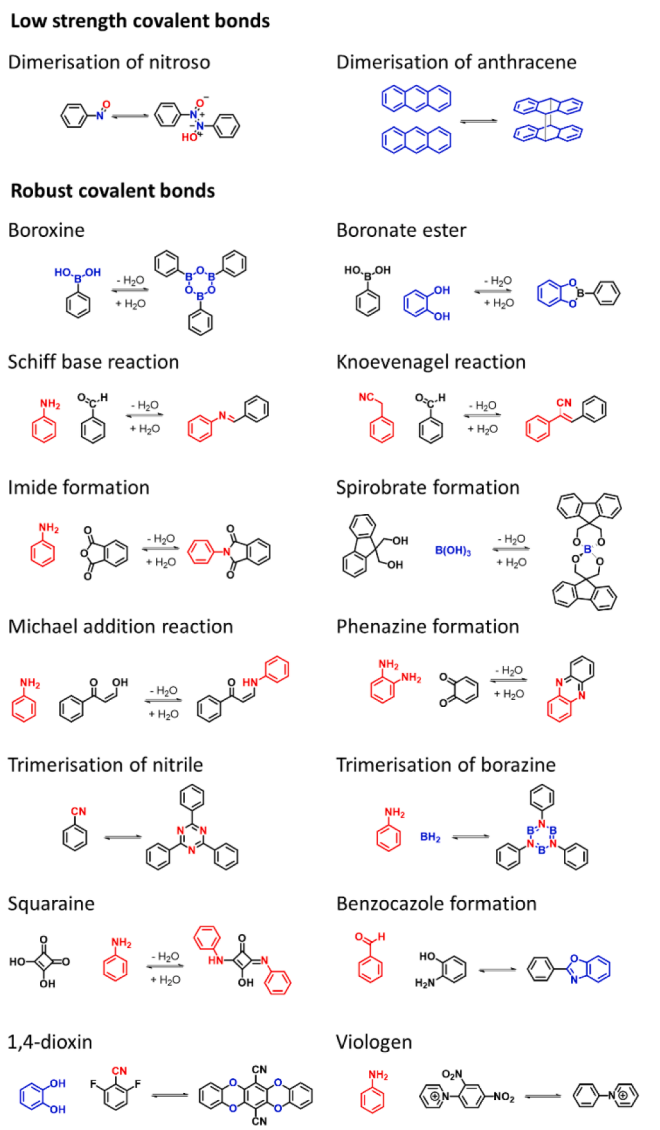

Fig. 3. Different types of reversible organic reactions used for COF construction. Adapted from reference 29 with permission of the copyright holders.

However, despite these linkage's higher stability and exciting properties, due to intrinsic reversibility, strong polarization, and several different synthetic strategies, the imine linkage is deemed a better choice than other dynamic bonds. It is important to mention the variation of the imine linkage to keto-enamine linkage by tautomerism equilibrium keto-enol (Fig. 5b). Thus, the favorable displacement of the equilibrium toward the latter tautomer improves the stability of the final structure since keto-enamine group is less reactive. This chemical conversion and locking of the imine bond represented a cornerstone for synthesizing new COFs [42].

Besides direct synthesis, the post-synthetic transformation of linkages is applied to synthesize novel ultrastable COFs. For example, benzoxazole-linked COFs (Fig. 5b) are constructed via a cascade reaction in which, after the reversible imine reaction took place, it was followed by cyclization via nucleophilic attack to form a benzoxazoline ring and, finally, the oxidation to benzoxazoline in an irreversible step [43]. The dioxin-linkers, whose production is based on irreversible nucleophilic aromatic substitution processes, are another pertinent reversible to irreversible transition bond (SNAr) [44].

To increase chemical stability against nucleophilic assaults and π -conjugation along the backbone, new research studies of ultrastable COFs have emphasized the C = C bond, e.g., cyanovinylene-based COFs [45]. Reversible Knoevenagel condensation was used to solve the problem of crystallizing a COF by reversible –CH = C(CN)- bond creation. One more extended conjugated backbone with excellent stability properties, the olefine-based COF, was achieved in 2019 and was prepared by an aldol-condensation of aldehydes and a highly electron deficient s-triazine core, the 2,4,6, trimethyl-s-triazine [46]. It is not easy to readily acquire the reaction conditions to make a COF, despite the variety of linkers allowing us to adjust our design network to a practical circumstance by modifying the COF stability. In the following charter, the many categories of synthetic conditions will be covered.

2.4. Synthesis of COFs

Most reported COFs are produced by solvothermal synthesis in sealed Pyrex tubes, combining the monomers in a suitable mixture of solvents. The building blocks are often unable to dissolve, so adding a catalytic agent is required before emptying and closing the vessel. The mixture is heated for days before the solid is separated, cleaned, and dried [16]. However, several variables significantly influenced the synthesis process, including pressure, temperature, reaction time, the volume ratio of different solvent combinations, and catalyst. There are significant batch-to-batch differences between COFs samples even after the optimum conditions are set.

Using aqueous acetic acid (AcOH) as a catalyst, the 1,4-dioxane: mesitylene combination undergoes the traditional solvothermal reaction to carry out imine-based COF at 120 °C [36]. Typically, it produces a powder that is unprocessable and unscalable. However, specific alternative synthetic procedures have been developed to address the shortcomings of standard circumstances.

Thus, several strategies have recently been devised to prevent reaction situations with high pressure and temperature. the more outstanding are room temperature [47], water [48], and sol–gel synthesis [49]. Although these strategies reduce energy/cost, they afford lower crystalline samples. Nevertheless, they have positive outcomes. Therefore, a growing interest is in developing sustainable and eco-friendly synthesis methods for COFs. While some green alternatives using non-toxic organic solvents have been reported, there are limited examples of energy-efficient and cost-effective methods that avoid using harmful solvents. A water-based synthesis method has been developed for β-keto-enamine-based COFs [50], but a general protocol for imine-based COFs is still required. Zamora and col. have successfully synthesized imine-based COFs in water using a limited amount of acetic acid at relatively low temperatures for five days. The reaction yield was pH-dependent, with the maximum yield obtained at a pH of 2.4 due to the degree of protonation/solubility of the amine monomer. Moreover, a microwave synthesis procedure was also used to reduce reaction time [48b].

On the other hand, the incompatibility of acidic conditions usually applied in conventional synthesis, generally by aqueous AcOH, a Brønsted acid catalyst, can be solved by alternative catalysts agents, e.g., basic pyrrolidine and Lewis acid metals. For example, scandium (III) catalyzed reactions readily proceed at room temperature, reducing the time of reaction to a few minutes and with low catalyst loading (2 % mol). However, its drawback is the versatility of different synthetic strategies, as it has difficulty constructing COF with specifically functionalized monomers [51].

A salt-mediated crystallization technique was then created using a new catalytic agent, which can address the scalability problem. P-toluenesulfonic acid (PTSA-H_2O) was introduced as a template and acid reactant, which helped build bulk-scale COF with high crystallinity and porosity [52]. The PTSA-amine salts served as a molecular organizer to create a lamellar structure with regularly spaced amines, whose dimensions are compatible with some routinely used aldehydes. This method allowed Prof. Banerjee and col. to produce a sizable family of COFs and transform them into macroscopic objects, including membranes, thin films, and foams. A different technique that involves

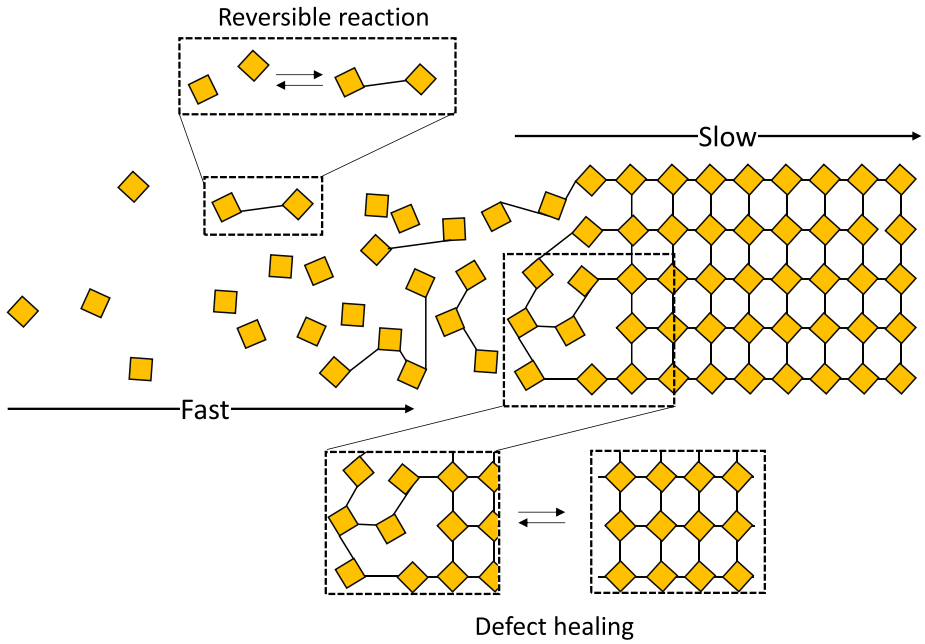

Fig. 4. COF production is reversible thanks to slow crystallization. An amorphous gel is first created, and as it slowly crystallizes. The production of imine COFs is consistent with this crystallization method. Adapted from reference 16 with permission of the copyright holders.

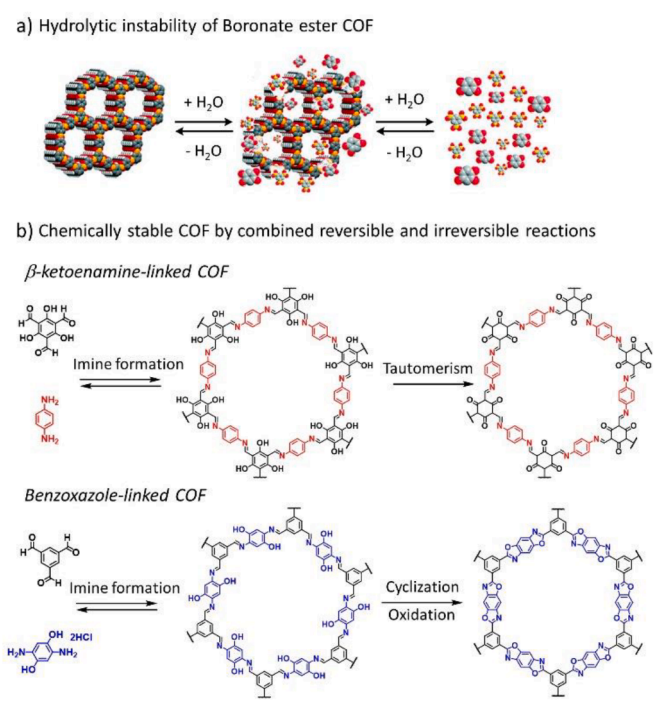

Fig. 5. A) diagram showing the hydrolytic breakdown of boronate ester cofs. b) combining reversible and irreversible processes to create very chemically stable cofs. adapted from reference 29 with permission of the copyright holders.

changing the reactivity of the initial building blocks can control the nucleation and growth rates by blocking the functional groups with a protective group such as *tert*-butyloxycarbonyl (Boc). The addition of the Boc group induces the development of low-soluble oligomers that allow for gradual growth as the deprotection activity develops [53]. The gradual deprotection enhanced the networks' crystalline quality, resulting in fewer nucleation spots that continue to grow.

The solvent is yet another crucial element that greatly impacts the synthesis reaction. Ionic liquids serve as both a catalyst and a solvent in this way. Furthermore, it produced remarkably crystalline material at high concentrations in minutes. Ionic liquids can be reused multiple times, but getting them out of the pores is still difficult [54]. This is one of the critical issues. The solvent-free approach, in contrast, has been helpful due to its straightforward and economical process. Due to its eco-friendliness, simplicity of use, and viability for scale-up synthesis, mechanochemical synthesis is a pertinent example. However, the limited crystallinity and porosity that these mechanically produced COFs displayed [55].

Because it can be challenging to achieve good structural order due to the intricacy of the building blocks, post-synthetic modification enables us to include functionalized building blocks that cannot be employed in traditional direct synthesis. Using a linker-exchange technique, for instance, it is possible to adapt simple networks created using the usual way to obtain previously unattainable COFs [56]. The linkers' reversible dynamic nature and their thermodynamically advantageous conversion created complex COFs with exceptional properties for cutting-edge applications. The following section will cover other post-synthesis functionalization instances.

2.5. Functionalization

The combination of various types of linkages and network topologies is undoubtedly important for network design, but it is essential to include functional groups in the framework because they offer extra features that allow the design COF to be specifically tailored to meet the needs of the intended applications. Furthermore, introducing an active moiety may impact the crystallinity and stability of COFs, making framework functionalization essential.

Pre-synthetic and post-synthetic alterations are two major categories into which functionalization methods for COFs can be divided. The first involves adding more groups to the construction blocks before combining COFs. The other tactic is centered on enhancing the existing COF structure. Adding a functional moiety to achieve a specific application or altering the linkage of the framework to increase stability are two examples of post-synthesis modification techniques.

The pre-synthetic method simplifies the monomers because the substrate is a tiny molecule. Functional groups, however, may impede the framework's development or become unstable under reactionary

circumstances. Post-synthesis alteration overcomes these limitations, resulting in a more complicated framework [57]. At the same time, it provides a method for creating crystalline, porous, and stable frameworks that cannot be produced using pre-synthesis techniques. Nevertheless, since the dispersion and functionalization of the reactants may not be complete, the structural change is more likely to produce faults.

The foundation of standard functionalization is a set of building blocks containing functional moieties that, in the first stage, do not obstruct COF growth and, in the second step, permit access to the target moiety. Therefore, the alkyne moieties that allow the network to be post-functionalized by click chemistry are the most representative functional terminal groups [58]. Additionally, even in gas–solid heterogeneous reactions, this active group can be changed into various moieties and modified by various reaction circumstances [57,58b].

Wang and col. reveal a rare instance of post-synthesis alteration by a functional group [59]. They demonstrated the planned synthesis of some 3D-COFs with various ethynyl group loadings. Notably, these alkyne-tagged 3D-COFs provide a platform for tailored click chemistry attachment of additional groups onto the framework. In the CO_2/N_2 separation, the pore surface engineering modification of 3D-COFs with various percentages of ethynyl groups was assessed. Since the functional loading density affects the adsorption selectivity for CO_2/N_2, 3D-COF-$[Ac]_{100\%}$ demonstrated about six times the selectivity of 3D-COF-$[Ac]_{25\%}$. Although the 3D-COF-$[Ac]_{100\%}$ reduced porosity size led to a lower gas permeability, it improved interactions with functional moieties and increased adsorption selectivity.

Post-synthetic functionalization, however, might not always call for the production of covalent bonds. By altering the structural links between COFs or offering a platform for integrating various molecules or immobilized metal ions, the structure of COFs can be modulated.

As described above, framework instability is resolved by post-synthesis modification techniques that convert the reversible link into an irreversible one (Fig. 6). One-pot reactions and post-synthesis modifications are two categories of structural locking alteration.

In the first one, the irreversible bond is formed through a series of reactions that occur entirely during the crystallization process, for example, keto-enol equilibrium that blocks imine-based COF into keto-enamine. A preliminary COF was needed for the post-synthesis modification, which is synthesized and separated traditionally. After that, a solid-state conversion event transforms the bond chemically into more durable molecules [17]. The conversion reaction is grouped into (i) chemical conversion linkages and (ii) linker exchange.

For instance, imine-based COF treated with redox agents can either

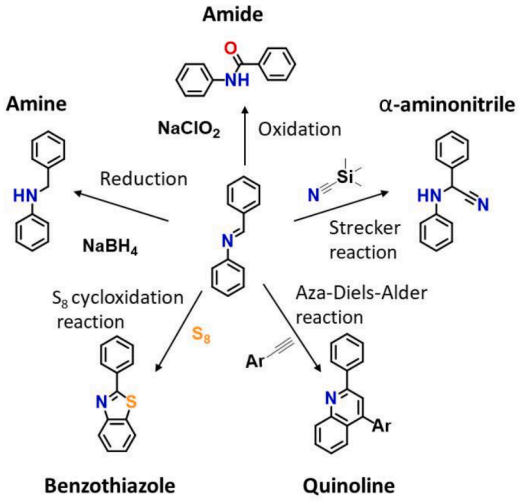

Fig. 6. Different irreversible processes were employed to lock the imine bond in COFs and produce the connection. Adapted from reference 32a with permission of the copyright holders.

be reduced to the second amine or oxidized to an amide linkage in the chemical conversion of links [60,61]. In that instance, a thiazole-based COF was topochemically created from a triphenyl triazine imine COF. Elemental sulfur combines with aromatic imine bonds at high temperatures, oxidizing to generate thioamides, which then combine to form a thiazole ring. Imine-based COFs are transformed into a sturdy connection by this post-synthetic alteration. Additionally, topochemical conversion alters the symmetry of the COF crystal, leading to the synthesis of novel COFs with chemical characteristics not possible with reversible reaction-based materials. This strategy, meanwhile, necessitates the employment of more severe response circumstances. Baek and co-workers reported employing 2,3-dichloro-5,6-dicyano-1,4-benzoquinone (DDQ) as an oxidant into benzoxazole links as a less harsh approach to overcome this problem [62].

However, since the linker exchange process is based on the foundations of reticular chemistry, a structural modification is always allowed as long as the building block exchange does not disrupt the symmetry and increases thermodynamic stability. This alteration can be accomplished under benign circumstances, garnering much scientific interest. According to Dichtel and col., this method shows how to obtain β-ketoenamine-linked COFs by substituting triformylphloroglucinol for 1,3,5-triformylbenzene [63].

As an alternative, the framework can be functionalized by adding metal ions. Regarding the various COF families, it is essential to note that imine- and amine-based COFs, which feature nitrogen-containing structures, may be alluring for introducing active metal ions due to their capacity for coordination [64], as reported by Wang and col [65]. in the functionalization of COF-LZU1 with Pd(II) to reach catalytic activity, the Suzuki-Miyaura coupling reaction is studied. COFs were used in other catalytic applications as templates to stop the ions in these metals from leaching and becoming inactive [66].

Although functionalization modifies the network to serve the intended function, other aspects improve the application's performance. The subsequent section will describe the essential qualities.

2.6. Properties of COFs

The impact of COF materials is determined by their distinctive properties, which are unique and inaccessible to other polymers and framework materials, such as low densities resulting from their exclusive composition of light elements (boron, carbon, nitrogen, and hydrogen) and their higher thermal and chemical stability, which is provided by the covalent bonds. We summarized the most outstanding characteristics in this section.

2.6.1. Crystallinity

Crystallinity is the key characteristic that differentiates them from other organic polymers. It is often assessed using structural modeling, Pawley or Rietveld refinement, powder X-ray diffraction (PXRD), and only very infrequently, single crystal diffraction [67]. As previously stated, one of the key components to achieving an ordered structure is the dynamic covalent bond, and the reaction's tuneability with the addition of modulators makes it possible to create highly ordered networks. In 3D-COFs, covalent contacts and their reversibility are the only factors that affect network formation. By reducing the chemical interaction of aldehydes with amines throughout the reaction and controlling crystal development in the case of COF-300, O. Yaghi and col. were able to produce the first single crystals of COF (Fig. 7) [67a].

Another method involves the planarity of monomers. By replacing the C-H moieties of the central ring in triangular building blocks with nitrogen atoms, the steric attraction between hydrogen atoms that causes the external phenyl rings to rotate was eliminated. This made it easier to stack the building blocks [68]. In contrast, it is also possible to synthesize highly crystalline and stable 2D-COFs via a non-planar approach. Stackable precursors may guide the stacking of the layer during growth with bowl- or armchair-shaped shapes, but their ligands

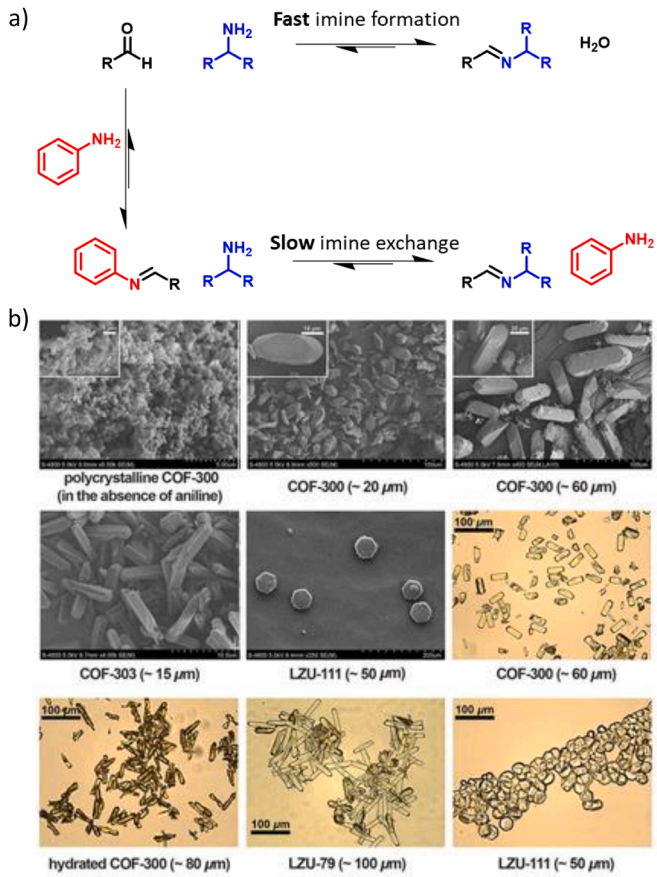

Fig. 7. A) without aniline, the equilibrium of imine formation is altered in favor of the end product, amorphous or polycrystalline cofs, whose formation is controlled by rapid nucleation and constrained crystal development. although the initial imine bond creation is relatively quick in the presence of aniline, sluggish imine exchange allows single-crystalline cofs to grow. b) images of single-crystalline cofs produced using scanning electron microscopy (sem) and optical microscopy in the presence of aniline, whose structures were clarified and solved in this research. for comparison, the sem picture of polycrystalline cof-300 without aniline is presented. adapted from reference 57a with permission of the copyright holders.

shouldn't have conformational freedom. In that regard, Mateo-Alonso and col. synthesized a highly crystalline 2D-COF with a wavy honeycomb structure using the building components 2,3,10,11,18,19-hexahydroxy-cata-hexabenzocoronene (HBC) (Marta-COF-1) [69]. The HBC adopts a twisted and hard shape, and due to the steric congestion between the hydrogens in the peripheral benzene rings, its conformational freedom is limited.

Even if the process increases the domain size of the nanocrystals over COF crystallization development, the synthesis typically results in a polycrystalline powder that PXRD can identify. Single-crystal X-ray diffraction (SCXRD) has only been used on a limited number of single-crystal COF instances to characterize them and determine their precise atomic structure and how it relates to their attributes [67a,70]. Alternative methods, such as advanced ab initio determination with cryo-continuous rotation electron diffraction, were used to precisely determine the structures of polycrystalline materials because the PXRD methodology was unable to fully comprehend the networks' structure (cryo-cRED) [71] or electron diffraction [67b].

The use of *ab initio* methods allowed Prof. Sun and col. to solve five difficult 3D-COFs at the atomic level utilizing examples of these tactics. Atomic precision is used to disclose the dynamic structures with flexible linkers, the degree of interpenetration, the position of functional groups, and guest molecules. The key to success is combining cryo-electron microscopy technology with hierarchical cluster analysis (HCA) [72], which increases the data completeness and redundancy for structure assessment and refining.

They were first ultrasonically dispersed in ethanol to transfer the meticulously prepared samples on a copper grid covered in carbon film. The sample was then cryopreserved to prevent structural expansion or contraction due to guest molecular adsorption or desorption and to fix the guest molecules inside the COF pores. Finally, samples were subjected to an ideal 3 and 0.5 sec duration to X-ray diffraction. Although the 3D COF chemistry is the primary focus of this study, the structure solution method provided a viable option to arrive at an accurate atomic structure.

As indicated, the stability and reversibility of the linker are adversely correlated with one another [17]. A decrease in stability can be seen since the covalent bond's reversibility made it easier to rectify network flaws with a higher degree of crystallinity. The part that follows will cover this subject. Because even strong bonds like boronate esters, imines, azines, or hydrazones can be hydrolyzed, the need for reversibility in COF linkage is the bane of chemical stability.

2.6.2. Stability

One of the most important qualities that researchers must consider for their desired application is the covalently bonded network structure, which plays a crucial role in the stability of COFs [15]. The analysis of the thermal stability and chemical stability of COFs constitutes the stability evaluation process.

Thermogravimetric analysis (TGA) revealed thermal stability up to 500 °C, not below 300 °C, and chemical stability is measured by a crude method, in which the solid is immersed in various solvents while being subjected to various conditions, quantifying the fraction of recovered materials and examining their crystallinity and porosity. The most

fundamental thermal and chemical stability trends have already been covered in the previous section; thus, just a synopsis will be made here. Therefore, pre-designed methods that entail a final, irreversible step through post-synthesis modification or are only reversible under extremely energetic circumstances are preferred for synthesizing highly stable COFs [73].

Since the section on functionalization discussed the importance of balancing stability, crystallinity, and complexity in COF, several techniques have been developed to increase strength without sacrificing crystallinity. Examples include hydrogen-bonding (H-bonding) interactions, which improve stability without harming crystallinity by locking the torsion of the edges and aligning the layer in one plane [74], by (π - π stacking's improvement. By adding hydroxy groups to the imine centers' borders, Banerjee and col. reported designing COFs with exceptional chemical robustness [75]. The COF demonstrated excellent chemical stability, maintaining its crystallinity for seven days in boiling water and 3 M of HCl (aq.). They tested the counterpart COF with methoxy-substituted and noticed worse chemical stability and crystallinity features to support further the idea proposed between chemical stability and H-bond interlayer interaction.

Chemical stability is often assessed by immersing the network in concentrated acids, bases, or water. However, stability can also have an impact on the porosity of the final product because interactions between the structure and solvent may cause the porosity of the material to be reduced. Therefore, robust structures guard against potential linker hydrolysis and porosity reduction.

2.6.3. Porosity

The structure of COFs was specifically designed to accommodate pore sizes ranging from 0.64 nm [76] to 10 nm [77]. Additionally, the stiffness of the framework permitted a porous construction, yet symmetry occasionally prevents access to the pore.

Typically, the dense clouds of monomers in 2D-COFs and the interconnected structures in 3D-COFs prevent these COFs from reaching their maximum potential porosity surface area of 3000–5000 $m^2\ g^{-1}$. Determining the maximal surface area requires careful activation and drying management, both of which are crucial. When the network is isolated, the capillarity strain contact of the solvent molecules with the network

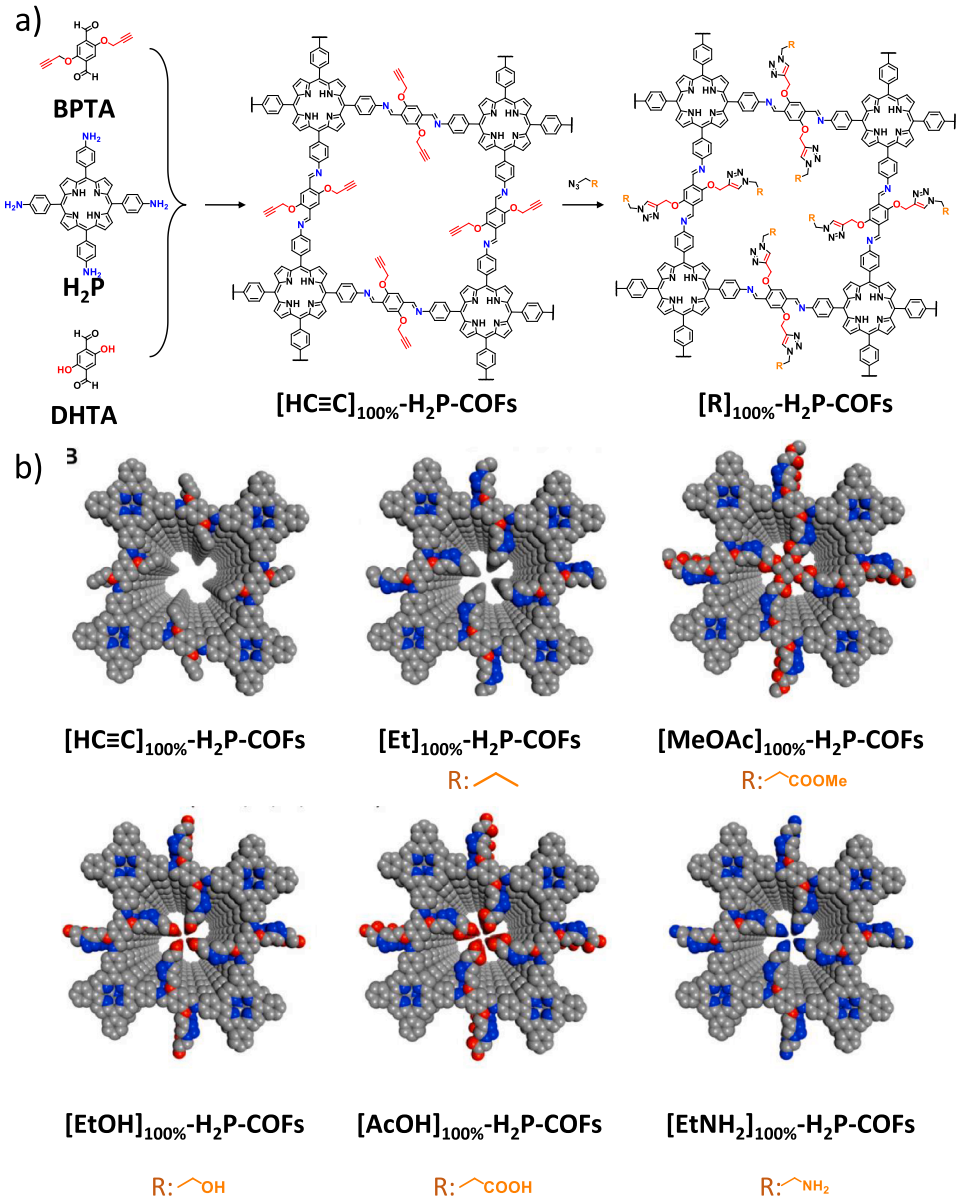

Fig. 8. Imine-based COFs' pore surface engineering schematic and their porous architectures with various functional groups are shown in the diagrams below (Gray, C; Blue, N; Red, O). Adapted from reference 78 with permission of the copyright holders.

causes a contraction of the framework, decreasing their porosity. Thus, efficient techniques are now being employed to prevent framework distortion [78], such as supercritical carbon dioxide (CO_2) and nitrogen (N_2) flow techniques during the activation process. The typical approach, however, varies from a solvent exchange to vacuum-assisted high-temperature evaporation of the materials.

Nitrogen adsorption at 77 K is frequently used to assess the porosity and cavity size of COFs. However, studying adsorption with additional gases can broaden our understanding of using them for gas phase absorption or separation. Due to their utility as energy sources or pollutants, hydrogen (H_2), carbon dioxide (CO_2), and methane (CH_4) are the gases whose consumption is most interesting [79]. By controlling the pore environment through functionalization with dipolar groups, adding metal nanoparticles, or reducing pore volume, it was possible to boost further the selectivity or capacity of uptake of these target gases [57]. For instance, Jiang's team used click reactions between azide compounds and ethynyl units to add alcohol, alkyl chains, carboxylic acid, ester, and amine units onto the pore wall of an imine-linked porphyrin COF (Fig. 8) [80]. Comparing functionalized COFs to alkyne COFs, pore surface engineering reduced the BET surface area, pore size, and pore volumes. For instance, when the number of ethyl units in comparing functionalized COFs to alkyne COFs, pore surface engineering reduced the BET surface area, pore size, and pore volumes. Thus, when the amount of ethyl unit in $[Et]_X$-H_2PCOFs was raised to 100 from 25, while the BET surface area dropped to 187 from 1326 $m^2\ g^{-1}$, and the pore size was reduced from 2.2 to 1.5 nm. The CO_2 adsorption capabilities, however, exhibited a distinct behavior.

Despite having similar tendencies to reduce BET surface area, pore volume, and pore size, ester units, hydroxyl groups, and carboxylic acid groups all displayed significantly greater CO_2 adsorption capacities than the ethyl group did. This was because they interacted with CO_2 more strongly than the latter. In contrast to cavity size, this example demonstrates how important the adsorption affinity between gas molecules and pore walls is. However, pore size control is critical for separation applications, where the target is not to maximize the adsorption of one molecule but to the difference in adsorption between two compounds. As such, several methods allow the formation of COFs with different pore sizes. The most straightforward one is the rational choice of the building blocks; by increasing their size, larger pores can be obtained in a family of isostructural COFs [81]. An alternative approach that allows reducing the pore diameter is the introduction of side chains in the building blocks that form the pore wall, this can be done either before the synthesis of the COF [82] or by post-functionalization reactions [57].

2.6.4. Electrical conductivity

In addition to the characteristics mentioned above, the electrical features of COFs are crucial for determining their applicability in optoelectronics and energy storage. However, COFs often have limited intrinsic conductivity and charge-carrier mobility, making it difficult to regulate their electrical and semiconducting properties [83]. Charge transport efficiency in conductive polymers is crucial and correlated with the degree of π-conjugation and molecular interactions. Nevertheless, it is still a significant synthetic difficulty to produce π-conjugated networks with high crystallinity. For 2D-COFs, the extended π-conjugation (in-plane) and π-stacking pathways are crucial for conjugation (out-of-plane) [83c]. The supramolecular assembly can alter the spatial stacking of monomers in the layered structures that produce electronic interactions, providing an interesting platform for adjusting their electronic characteristics. Triazine, hydrazine, azine-linkage, and other compounds are investigated for increased electrical conductivity since spatial stacking is typically adjusted by bond polarization [84].

Using remarkable methods, conductive 2D-COFs have been constructed using the Knoevenagel condensation-produced C = C bond [85], having conductivities up to 10^{-4} S cm^{-1} that improve electron delocalization. In addition to bond polarization, structural alterations, including lengthening linkers, incorporating impurities, doping, and intercalating transition metals, can be used to tune the electrical conductivity [86]. Large conjugated and planar construction components provide the basis of most semiconducting COFs such as triphenylenes [87], pyrenes [88], three-dimensional tetrathiafulvalene [89], porphyrins [83b] and phthalocyanines [90]. Furthermore, charge transfer through and between layers is enhanced by the favored π-orbital overlap seen in planar building blocks.

Alternative conjugated systems can be made by constructing composites of graphene, carbon black, carbon nanotubes (CNTs), and carbon fibers and enhancing conductivity (Fig. 9) [91]. For instance, Jiang and col. [92] show how to fabricate crystalline, mesoporous COF that is redox-active for use as electrodes. Growing COFs on CNTs considerably increases electron mobility, and the open porous CNT structures further facilitate the passage of ions to the reaction sites. These structural characteristics and physical traits work together synergistically to create COF-based cathodes that effectively use the redox-active units, display strong cycle stability, and promote high-rate energy storage and power supply.

2.6.5. Catalytic activity

They were able to create regular channels due to COFs' crystalline and customized framework, which has garnered much interest for heterogeneous catalysis. As a result, the basic design of COF walls can be employed either immediately or after being functionalized with metal. Ding and coworkers reported the first instance of using metal moieties in COFs for catalysis, coupling Pd-species from $Pd(OAc)_2$ [65]. The Suzuki-Miyaura coupling reaction was catalyzed by the resultant Pd@COF-LZU1.

The framework of COFs has also been successfully used as catalytic agents, as opposed to tweaking structures with metal species. For instance, a β-ketoenamine COF that dehydrates fructose with high chemo-selectivity has sulfonic acid groups at the pore walls [93]. Chiral catalysis is another intriguing form of catalysis, however, thus far, very few COF structures have been found. For instance, Jiang and col. [58a] described the creation of a chiral mesoporous imine-based COF using click-chemistry after adding a chiral center ((S)-2-(azidomethyl)pyrrolidine) with organocatalytic activity. The resulting solid, metal-free structure is a test case for showcasing the COFs' potential in asymmetric catalysis.

Finally, their potential photocatalysis performance has been investigated because of COFs' outstanding visible light absorption, adaptable band gap shape, and quick electron-hole separation and transfer. Since Prof. Lotsch and col. reported the first discovered example, interest in COF-based photocatalysis has surged significantly [94]. The major uses are photocatalytic H_2 evolution, O_2 evolution, CO_2 photoreduction, and photodegradation of contaminants. COF-based photocatalysis is a beautiful response to the pressing need to create clean, renewable energy sources, convert CO_2, and degrade environmental pollutants [95].

2.6.6. Luminescence and photovoltaics

Multiple π-conjugated monomers can be combined thanks to the modular character of COFs, but good quantum yields require strong linkage dependence in the structures. For instance, in imine-based COF, rotational and vibrational relaxation routes can result in non-radiative decay. However, using highly fluorescent subunits, like anthracene, also makes the imine bond more planar and circumvents the non-radiative decay processes [96]. Pyrenes and triphenylenes are two more prominent subunits utilized to create luminous COFs. However, the unpredictable chromophore-containing COF architectures and the scarcity of monomers for luminescence restrict the creation of luminescence COFs, which are still under study [97].

To increase the effectiveness of charge separation for photovoltaic systems, it is crucial to build segregated networks of donor and acceptor groups. Conventional methods typically needed extra units to start other

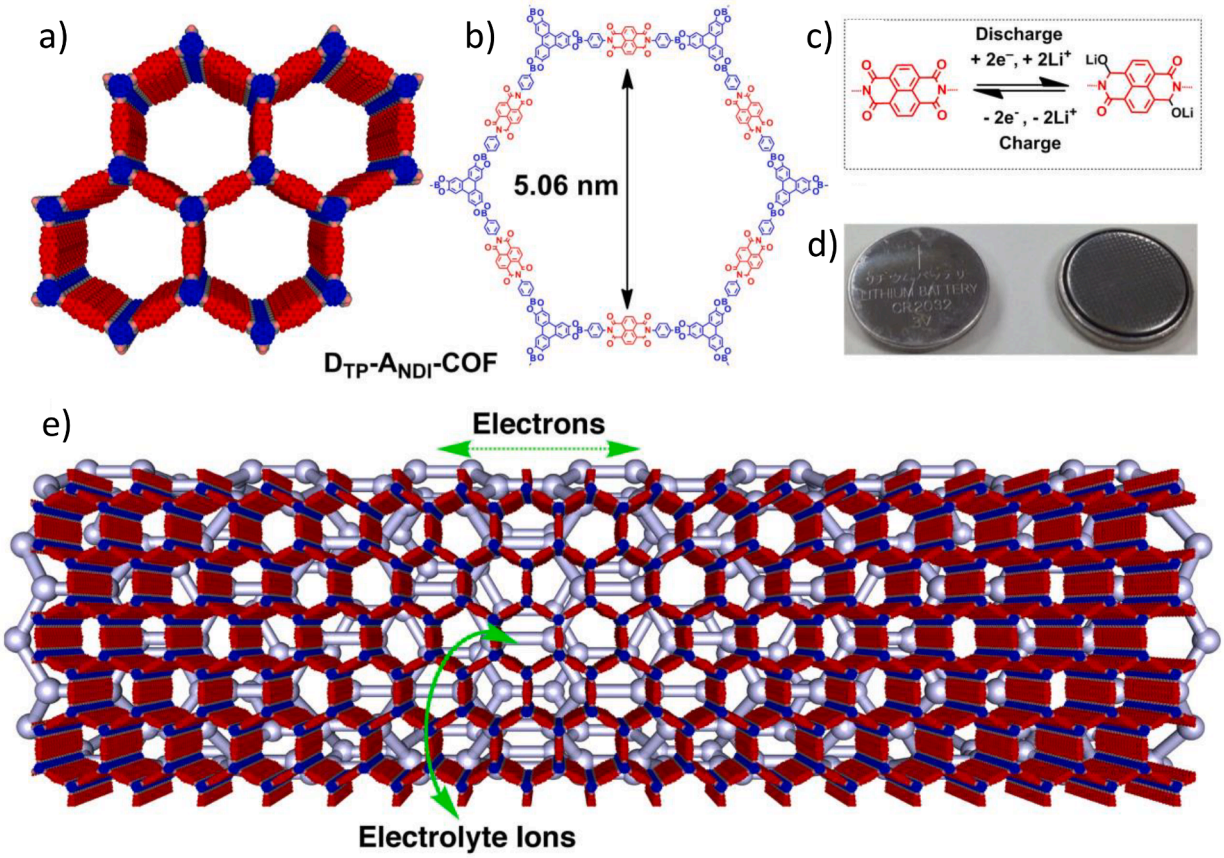

Fig. 9. Diagram of the DTP-ANDI-COF AA-stacking with one-dimensional *meso*-scale channels and red walls made of redox-active naphthalene diimide. b) The chemical composition of a single DTP-ANDI-COF pore. c) The naphthalene diimide unit is undergoing an electrochemical redox process. d) Images of coin-style batteries. e) A graphic depicting electron conduction and ion transport in DTP-ANDI-COF@CNTs (grey for CNTs). Adapted from reference 80 with permission of the copyright holders.

interactions powerful enough to cancel out the electrostatic force to make that assembly possible. The creation of alternate donor-on-donor (D-D) and acceptor-on-acceptor (A-A) (π columnar structures without the usage of any additional units) COFs was made possible by the topological design of donor–acceptor COFs (D-A COFs) [98]. Their distinguishing characteristics are the covalently connected network that facilitates photoinduced electron transfer and the D-D and A-A (columns that provide a channel for carrier transport) features of D-A COFs systems. Jiang described a kind of D-A COF in which zinc phthalocyanine donor knots (DZnPc) condense with electron-accepting naphthalene diimide linkers (ANDI) to form D_{ZnPc}-A_{NDI}-COFs [99]. Time-resolved spectroscopy was used to analyze the charge dynamics of D_{ZnPc}-A_{NDI}-COFs, revealing an ultrafast electron transport from the donor to the acceptor columns. Additionally, the outstanding long-term charge retention and quick charge separation gave mechanistic insight to see the enormous potential of D-A COFs for photoelectric applications.

2.7. Processing of COFs

Integrating COFs in devices is still difficult despite the remarkable qualities highlighted above and its features, including personalized design, persistent porosity, and long-range order. Most documented synthetic COF techniques for COFs use solvothermal conditions, resulting in fully insoluble powders and randomly arranged crystallites. Because COF powders are difficult to process, they cannot be utilized in the technologies that are now in use. Therefore, it would be advantageous to create novel synthetic and processing techniques for COF production that would enable COFs to be shaped, positioned, and oriented according to requirements.

2.7.1. Engineering shaping of COFs

New synthetic techniques have been devised to create macroscopic COFs structures that may be used in advanced applications with additional support or on their own [100].

Novel synthesis approaches are linked to ways of producing COF objects without further support [101]. According to Banerjee and col., the first instance of molding COFs was mixing amine with p-toluenesulfonic acid in the first stage. After that, it was blended with aldehyde and water to create a dough that, when baked, formed a very porous and crystalline substance [52]. This approach allowed for the large-scale, continuous extrusion of a wide range of centimeter-sized parts utilizing molds. This method was modified by reacting sodium bicarbonate ($NaHCO_3$) with p-toluenesulfonic acid to produce constant CO_2 effervescence, which allowed the development of 3D-hierarchical disordered nanostructures, or COF-foams, in which micro- and macropores coexist. Applications for COF-foam include quick removal of various pollutants and ionic diffusion through electrodes in electrochemical cells due to the variety of pore sizes available [102]. It has been claimed that certain synthetic methods, such as generating lightweight macroscopic COF-aerogel from gels, can produce hierarchical porosity in COFs.

To find an engineering shaping protocol of reaction that allows shaping COFs into macroscopic objects, Zamorás group also reported an outstanding procedure, using acetic acid as a reaction solvent, to produce COFs-gel at mild conditions in second due to catalytic excess. Acetic acid was used as a catalyst and solvent, and the building blocks were gelled immediately without using binders or solvothermal processes. The reaction mold's form was preserved during the soft activation of COF gel by supercritical CO_2 drying, and the resulting macroscopic COF aerogel featured a hierarchical porosity from

micropores to mesopores and macropores, demonstrating an outstanding adsorption capacity [49]. The quasi-immediate jellification and numerous nucleation locations produced a macroscopic entity made of randomized COF nanolayers. Additionally, a sponge-like network made of COF nanolayers with a fiber shape formed the hierarchical porosity.

Several methods for building sturdy macroscopic COF objects have been created using a template. For instance, Banerjee and col. used 3D printing to construct 3D macro-architectures of composites GO@COF foams using the dough form with a mixture of p-toluenesulfonic acid, monomers, water, and graphene oxide as an ink (Fig. 10) [103]. Graphene oxide, reduced graphene oxide [104], chitosan [105], and Pluronic F127 [106] are illustrations of templates for building macroscopic COFs.

Puigmartí-Luis, Zamora and col. described the preparation of fibers from an imine-based COF with excellent structural order using a microfluidic chip establishes a precedent to produce many different materials utilizing this reagent mixing technique, which offers novel materials that are difficult to obtain using bulk processes. A highly crystalline and porous covalent organic framework made up of fibrillar micro-structures is created when 1,3,5-tris(4-aminophenyl) benzene and 1,3,5-benzenetricarbaldehyde react in acetic acid under continuous microfluidic flow conditions. The COF fibers have mechanical stability that enables direct 3D drawing of objects on several surfaces [107].

2.7.2. Thin film

Compressing the insoluble powder material to create membranes is the simplest processing method, however, using too much pressure might cause structural damage. Membranes can be built to stop it thanks to a delicate balance between the pressure being exerted and the porous network's fragility. Additionally, according to Uribe-Romo, a rising stacking order was seen during the alignment of COF layers [108]. However, the large thickness and irregularly aligned COF powder prevented a full availability of COF moieties [109]. For further practical applications, novel techniques for creating COF thin films are also imperative. Both bottom-up and top-down approaches can be used to fabricate COF thin films.

The bottom-up methodology was the main strategy that allowed COFs to be deposited on substrates with a controllable dimension of thickness and surface.

Four primary methods have been used to fabricate COF thin films on different interfaces or substrates: interfacial polymerization, solvothermal synthesis, synthesis under continuous flow conditions, and room-temperature vapor-assisted conversion.

Various methodologies have been reported in which the synthesis of single and few-layer COFs in ultra-high vacuum was achieved by evaporating the building blocks and polymerizing over a metal surface or graphene layer. For example, the growth of COF films on single-layer graphene via bottom-up strategy under solvothermal conditions showed an improved crystallinity due to the high preferential orientation towards lying with the stacking direction perpendicular to the substrate over COF-powders, which are ideal for organic device applications [110].

However, solvothermal synthesis requires an alternative technique in moderate settings since it produces fragile monomers vulnerable to harsh temperatures. To circumvent this problem and build COF thin films using fragile precursors on delicate substrates, Bein and col. reported a mild condition vapor-assisted conversion. The process involved mixing a monomer combination and drop-casting it onto a glass substrate. Next, the substrate was placed in a desiccator with a mixture of mesitylene and dioxane, whose vapors improved the crystallinity and produced the COF thin film. Notably, the concentration and droplet volume can influence the thickness. The COF thin films' thickness might be lowered to 300 nm [111].

Flow synthesis can be used to evolve the control over film growth further [112]. The system comprises a thermostatically regulated chamber in which a solution of the various monomers flows via a tube with specified dimensions against the substrate before exiting the system along its edges. By adjusting the residence duration, this technique produced a more uniform film and independently enhanced crystallinity and thickness.

Alternative techniques are required to produce free-standing thin films with vast areas because the substrate's dimensions constrain the thin film's size. Therefore, an interfacial technique that involves the

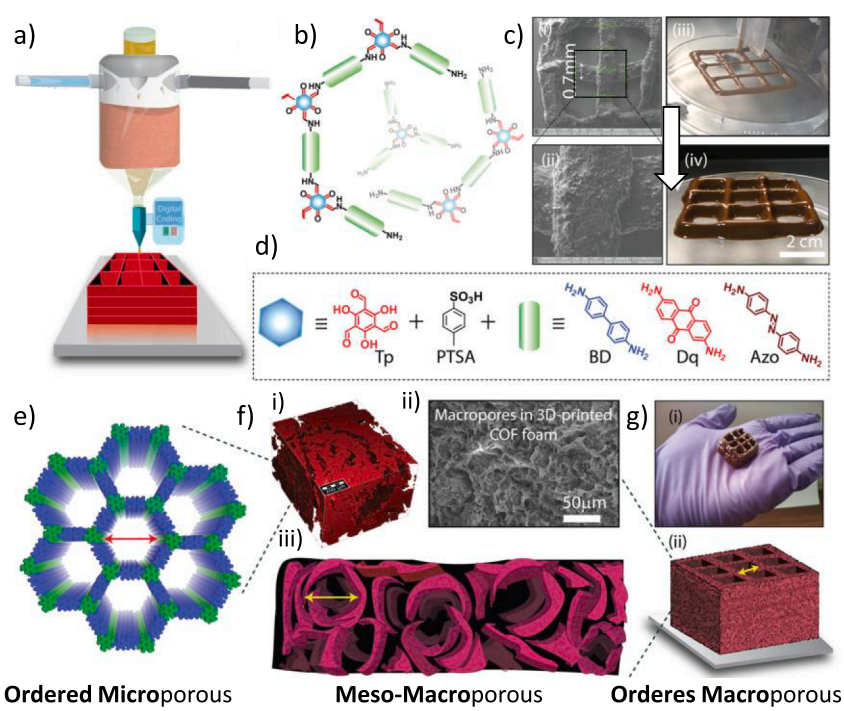

Fig. 10. A) illustration of the cof-go foam synthesis and 3d printing process. a hydrogel is created when graphene oxide, water, and cof precursors are combined. this hydrogel is employed in 3d printing. b) schematic depiction of the cofs' incomplete frameworks. at this point, we anticipate that the 3d printing ink will begin to form oligomers or incomplete framework structures. c) (i,ii) the sem image of a cof-go foam grid that was 3d printed at a millimeter scale with a print resolution of~ 0.7 mm and pore size of ~1.5 mm. c) (iii, iv) The digital images of a COF-GO foam grid that was 3D manufactured at a centimeter scale. d) The ingredients used to create COF-GO foam. e) The TpBD COF space-filled model. X-ray microtomography of TpBD foam created via 3D printing. It exhibits the macropores in the matrix of the COF-GO foam, the macropores in the matrix of the SEM picture of the TpBD foam monolith, and the macropores in the matrix of the graphical representation of the macroporous foam. g) A graphic representation of the nine-pore COF-GO foam grid and I a digital photograph of a 2.3 × 2.3 cm self-supported nine-pore COF-GO foam grid that was 3D printed. Adapted from reference 91 with permission of the copyright holders.

interaction of several monomers at a constrained interface area, where the growth of thin film is regulated in one direction, allows for the synthesis of large-scale thin films. Three different types of interfaces have been used: liquid/air, liquid/liquid, and liquid/liquid/gel triphasic. However, it is still difficult to show the structural order in such thin materials, and STM images provided the only evidence of connection formation [113].

Recently, Prof. Zheng and col. created a unique synthetic method to produce thin films at the liquid/air interface that are 2D-COF orientated. Poly(sodium 4-styrenesulfonate) (PSS) was dispersed at the air–water interface to produce massive single crystalline domains. The 2,5-dihydroxyterephthalaldehyde-induced polymerization and crystallization of the protonated building blocks 5,10,15,20-tetrakis(4-aminophenyl)-21H,23H-porphyrin (TAPP) were directed by PSS (2,5-Ph). P-toluenesulfonic acid monohydrate (PTSA) protonated the TAPP monomer, and electrostatic interaction between PSS and TAPP directed the ordering and accumulation of the TAPP. However, another significant crucial component was the concentration of ethanol, which made 2,5-Ph more soluble and reduced water's surface tension, allowing for the diffusion and assembly of molecular species. Thus, it was demonstrated that preorganized monomers under PSS and their diffusion oversaw producing 2D-COF oriented thin films.

Two non-miscible liquids are used to create the interface at the intersection in liquid/liquid interfacial polymerization. For instance, Dey and col. successfully created a novel synthetic technique to build large-scale COFs of β-ketoenamine thin films at the interface of water and dichloromethane. While aldehyde is contained in the dichloromethane solution, PTSA, the reaction's catalytic agent, protonates the amine-containing water solution. The reaction is restricted at the interface because neither the aldehyde nor the protonated amine is soluble in water or dichloromethane solution. The thickness can be as thin as 50 nm and is modulated by the concentration of the precursors. Additionally, COFs thin film is easily transferable to other substrates while maintaining the crystalline structure and its physical shape [114].

Finally, a liquid/liquid/gel triphasic system utilizing hydrogel produced a different method (Fig. 11). Drops of water are introduced to the system when a hydrogel is immersed in oil, and a super-spreading water layer is created. One of the monomers was added to the gel, and the

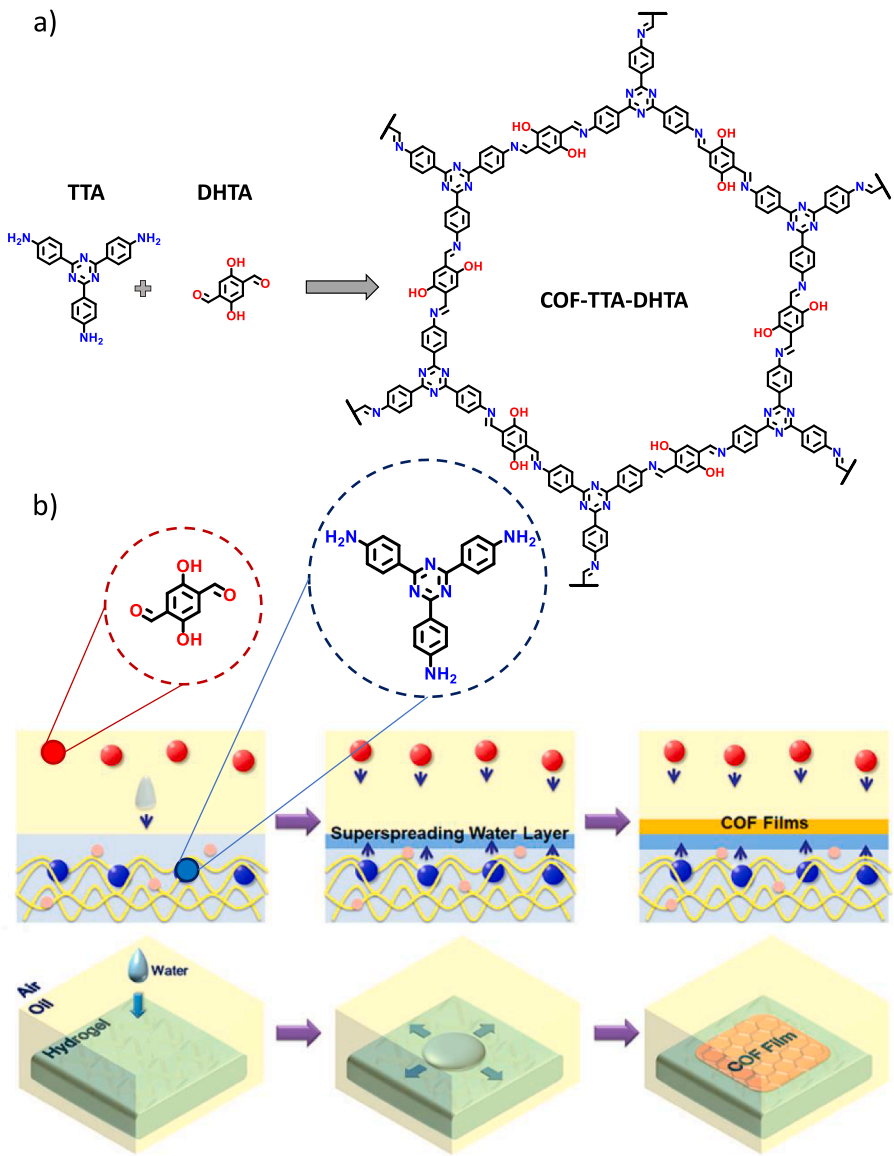

Fig. 11. A) the chemical compositions of COF-TTA-DHTA, DHTA and TTA. b) a schematic showing how thin cof films can be made at hydrogel surfaces using constrained super spreading water layers underneath the oil. adapted from reference 102 with permission of the copyright holders.

other was dissolved in the oil phase to form a thin film. The concentration of the building blocks was changed to alter the thin film thickness between 1.8 and 200 nm. Because thin films could be transferred to silicon substrates with holes imprinted, their mechanical properties could be evaluated using nanoindentation [115].

A different approach to the organic/water interface used $Sc(OTf)_3$ to encourage imine production and control polymerization there. Site-selective polymerization is made possible by separating the catalysis, in which the monomers remain in the organic phase, and the Lewis acid catalytic agent in the aqueous phase. This results in a thin film at the interface [116].

In contrast to the bottom-up approach, the top-down approach calls for the production of free-standing, single- or few-layered COF thin films from bulk materials as opposed to growing precursors on particular substrates or interfaces. Covalent linkages, which preserve the layer structure, and interlayer interactions in the layer's vertical direction, such as the Van der Waals force and/or hydrogen bonding, are the two forces that often regulate 2D-COF crystals. To separate COF layers without causing harm, the exfoliation process relies on disrupting π - π stacking interactions by internal or external force in the form of ultrasounds.

Motivated by the effective graphene exfoliation [117] and other monoelemental 2D materials such as antimony [118] and black phosphorous [119], Zamora and col. obtained for the first time delaminated covalent organic nanosheets (CONs) by simple sonication of bulk laminar COF-8 in dichloromethane. The thickness, measured with atomic force microscopy (AFM), of the CONs was 4 nm corresponding to approximately ten layers [120]. Liquid phase exfoliation (LPE) and micromechanical exfoliation are the two most used techniques for COF exfoliation (MME). The solvent trapped between the flakes by ultrasounds causes delamination of the bulk material, which is advantageous for the liquid phase exfoliation process. Two of LPE's key disadvantages are large faults and low yields.

In contrast, the so-called Scotch tape method, mechanical exfoliation (MME), involves crystal delamination using adhesive tape. The most well-known example was graphene, which Geim and col. originally isolated in 2004 using the Scotch tape technique [121]. To lessen the thickness of the layers created, repeat the operation numerous times. MME might not be the most effective procedure when dealing with polycrystalline materials; instead, ball milling or mortar can be employed. Both methods are intriguing for getting exfoliation with less harm. However, it has several significant flaws, including a low yield and a high price, making it technologically obsolete. There are no known examples of COF crystals that are appropriate for MME. However, CONs with some crystallinity were produced by mechanical grinding exfoliation in the presence of a few drops of solvents, and their thickness range was about 3–5 nm (10–15 layers) [122].

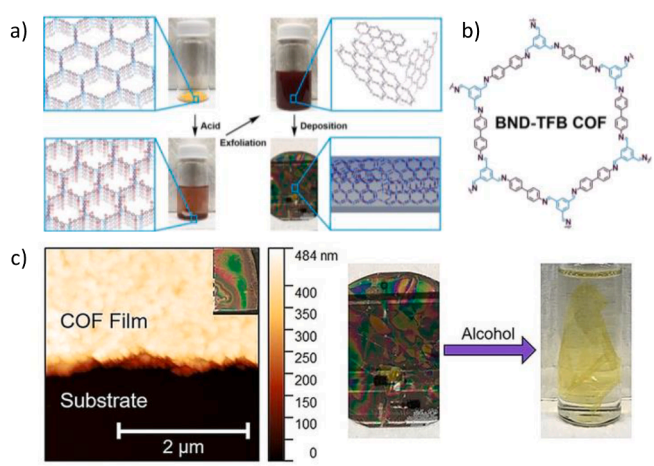

Fig. 12. A description of the film casting and acid exfoliation techniques. Electrostatic repulsion caused by protonation of imine-based COF particles causes fast exfoliation of the powders into thin sheets when stirred. Exfoliated COF sheet suspensions were applied to substrates, dried, and formed into thin crystalline COF films. b) The porous design of the BND–TFB COF. c) An AFM image of a 400 nm-thick film's edge and images of a film taken before and after reagent alcohol delamination. Adapted from reference 111 with permission of the copyright holders.

By using chemical exfoliation techniques like a post-synthesis modification or protonation of the framework, new methodologies exclusively attempt to disrupt π-π interactions between stacks of molecules [123]. A method for exfoliating imine-based that can be scaled up was disclosed by Dichtel and col. Trifluoroacetic acid (TFA) was used to protonate the imine bond during the exfoliation process, which disrupted the stacking interaction and allowed for dispersion into organic solvents but also changed the crystallinity and porosity of the COF [124]. The exfoliated solid was separated in the first step by centrifugation and then dried by vacuum after being stirred with a different solvent mixture to remove TFA. A continuous thin film was created when the exfoliation suspension was deposited onto a silicon wafer and air-dried. The resulting thin sheets were around 400 nm thick (Fig. 12). Intriguingly, the thin film can also be separated off the silicon wafer to create a free-standing thin film that can be applied to any desired support. As a result, acid exfoliation can be used as a powerful technique to prepare COF powder based on imines for practical applications.

2.7.3. Particle and nanoparticle morphology

The only processing methods available to develop some sophisticated applications are COFs molded into macroscopic objects, membranes, or thin film construction. Researchers have paid close attention to materials that are modulable in size and shape, such as nanosized or nanomorphology (Fig. 13), because they are more appropriate for specific applications such as catalysis, separation, sensing, drug delivery, and energy storage [125].

One of the most basic shapes is the sphere. But until Wende and col. recently published a size-controllable synthesis of uniform spherical COFs from nanometer to micrometer scale by a simple technique at ambient temperature, control over the morphological size and diameter was not resolved [126].

More recently, Maspoch and col. have described a very adaptable and powerful way for fabricating microspherical hollow imine-based COF superstructures while simultaneously shaping them. The approach combines the spray-drying methodology with a dynamic covalent chemistry process. This technique has created COF-based composites by simply including the chosen functional components during the spray-drying synthesis [127].

The spherical COFs are chemically and thermally stable and have a large surface area. During manufacturing, the building components were combined with acetonitrile (ACN) and acetic acid (AcOH) solutions. The outcome suggested that the amount of AcOH may be used to influence the spherical COF size. Due to Ostwald ripening of initially produced spherical aggregates of COF crystallites, it was shown that the hollow spheres alteration of the spherical morphology was feasible under solvothermal circumstances [128].

Anisotropic COF morphologies, such as hollow tubular COFs, can also be created. The construction mechanism used zinc nanorods as a template to grow the organic framework [129]. Zinc was eventually removed from the composite material through an etching reaction with aqueous acid; hence the manufacturing required acid-stable COFs. Our team recently published a one-pot synthetic method that, under mild conditions, produces stable aqueous colloidal solutions of sub-20 nm crystalline imine-based COF particles, pushing the size limit even lower. Additionally, the colloidal solution can be transformed into 2D and 3D COF shapes using this technique, by a COF ink that can be printed directly onto surfaces [48c].

Preparation of COF nanosheets (CONs) is a suitable way to overcome

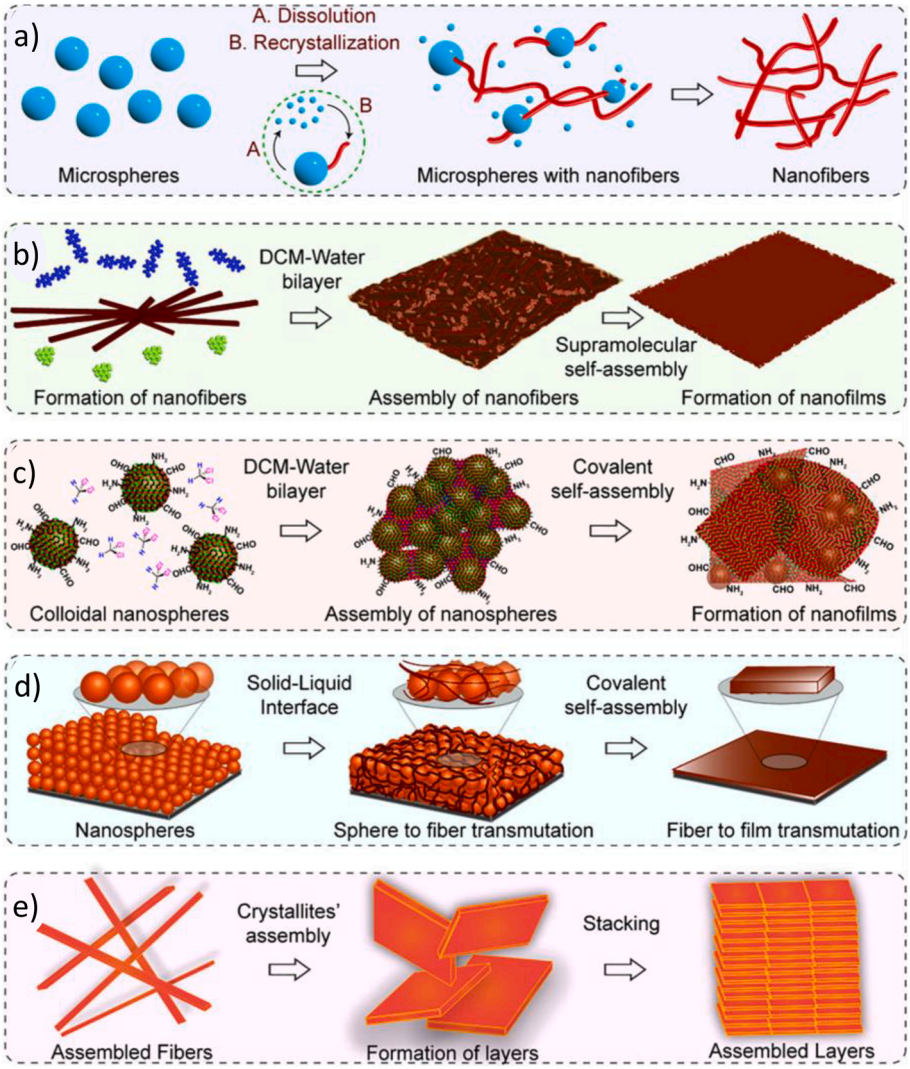

Fig. 13. Transformation of COF morphologies to their respective dimensionalities, such as a) from 0-D (COF microspheres) to 1-D (COF nanofibers) via dissolution–recrystallization of COF crystallites. b) during interfacial crystallization, from 1-D (COF nanofibers) to 2-D (COF thin films). c) Through mesoscale covalent self-assembly, 0-D (COF nanospheres) to 2-D (COF thin films) conversion. e) 1-D (fibers) to 2-D (sheets) to 3-D (membranes) via slat-mediated gradual baking of molecular building blocks. d) 0-D (COF nanospheres) to 1-D (COF nanofibers) to 2-D (COF thin films) at the solid–liquid interface. Adapted from reference 112 with permission of the copyright holders.

their processability limitations and enable their use in some scenarios, as it is the case of biomedical applications that require materials with nanometric dimensions or some catalysts that use as active sites the atoms located at the border of the nanolayers [130]. Using CONs in membranes and other applications is a promising field of study, and ongoing research is focused on improving their performance and scalability [131]. The rational selection and combination of molecular precursors already provide CONs with a large variety of properties. For instance, photoluminescence, electrode modification, sensing, capture of pollutants, energy storage, (electro)catalysis or separation, therefore, CONs have already been pointed as materials for several applications and devices.

One of the most promising applications for COFs is their use as membranes for separation in both liquid and gas phases. Ultrathin COF membranes, i.e., sub-1 μm-thick, are required to achieve this [132]. The controlled thickness of CONs allows modulation of COF material properties by making it dispersible in solvents, enhancing performance in various applications.

Additionally, CONs can be growth on specific supports. Thus, 3-aminopropyltriethoxysilane and 4-formylphenylboronic acid can be functionalized alpha-alumina supports to prepare boronic acid groups on the terminal surfaces. A COF-5 layer can be formed on the support using a condensation reaction, but this approach has limitations due to the formation of defective layers. A continuous method has been developed to produce a 400 nm-thick COF-LZU1 layer on alpha-alumina support, which can be used as a molecular sieving membrane [133].

Downsizing COFs to CONs can enhance their physical properties, such as improving their fluorescence [134], which can be used to detect organic pollutants in water [135]. Moreover, COFs have been utilized for their CO_2 capture properties in developing a cathode catalyst for Li-CO_2 batteries. An imine-based COF was grown as a nanometer-thin film, based on CONs, directly on a graphene surface. The polar C = N groups of the COF enhanced CO_2 adsorption, resulting in CO_2 nano-enrichment and nanoconfinement. This improved the efficiency of the Li-CO_2 battery by reducing polarization and cycling issues [136]. Additionally, using CONs in lithium-ion batteries improves their performance by allowing almost all redox-active sites to participate in the electrochemical process. Finally, CONs prepared at the liquid/liquid interface have shown promise as nanofiltration membranes for separating rhodamine WT from aqueous solutions, demonstrating high rejection percentages of 91% [116].

2.7.4. Hybrid materials

Another processability technique, in addition to the shape and morphological control, is mixing various materials or COFs with other functions that could have synergistic benefits. Examples of properties that have been improved include electrical conductivity, gas selectivity, and alteration of growth orientation. For instance, the structural arrangement of carbon nanotubes (CNT) used in the synthesis of COF prevented COF accumulation and increased structural order [137]. The

covalent interaction with CNT also enlarged the composite's π-conjugation system and enhanced electrochemical sensing application and electrical conductivity.

Covalent bonding is a common technique for creating hybrid materials, therefore, a functionalization of the surface is necessary. These methods can be used to create hybrid materials with alumina oxide (Al_2O_3) [133b], silica [138], or MOFs [139]. For example, NH_2-MIL-68@TPA-COF, the first reported MOF@COF core–shell hybrid material [139b], was an efficient organic pollutant degradation photocatalyst driven by visible light. Tris(4-formylphenyl)amine (TFPA) was used to functionalize the original MOF, NH_2-MIL-68, which had a rod-like morphology. The resulting compound, NH2-MIL-68(CHO), still had the same morphology. The MOF@COF core–shell hybrid material was then produced by condensation of TFPA and tris(4-aminophenyl)amine (TAPA) in a combination of NH_2-MIL-68(CHO). The MOF@COF core–shell demonstrated greater photocatalytic activity, around 1.4 times more than NH_2-MIL-68. This increased activity of the hybrid material compared to the pure MOF may be attributed to the reduced band gap and better BET surface area.

2.7.5. Membranes

As indicated above, manufacturing membranes is the most typical way of processing COFs. COF membranes have shown numerous breakthroughs in separation applications because of their simple operation, low cost, and environmentally friendly production, even though the thickness is still a disadvantage compared to COF thin film [140].

Membranes can be categorized by their constituent parts into two main groups: mixed matrix membranes (MMMs) and pure membranes.

The porous fillers can be blended into a polymeric matrix solution to prepare the MMMs. In a ground-breaking study, Banerjee and col. created a solution of spherical COF nanoparticles that resembled flowers and were then mixed with a polymer matrix (PBI-Bui) to create a self-supported hybrid membrane.

The organic makeup of COF nanoparticles and their H-bonded interaction with the benzimidazole groups of PBI increased the permeability of the composite matrix. This allowed the membranes to exhibit flexibility and high thermal and chemical stabilities, a crucial need for real-world applications [141].

The casting methods may include a prior exfoliation step, mechanical grinding, or morphological shaping to improve the diffusion into the polymer matrix. Using COF layers to cover porous support is another way to create MMMs. Although bottom-up methods are ideal for membrane generation, most CONs are prepared by top-down methods because of their scalability. However, CNOs can be incorporated into mixed matrix membranes (MMMs) to improve their hydrogen permeability while reducing carbon dioxide permeability, thereby enhancing H_2/CO_2 separation performance [142]. However, current methods for preparing COF membranes are still limited, and most so-formed membranes have defects that limit their use in separation applications.

Additionally, MMMs can be formed using CONs suspended with graphene oxide and passed through a cellulose acetate filter. Due to the stronger interactions between graphene oxide and COFs during filtration, both materials were restacked to cover the cellulose acetate filter. The interlayer channels grew more constricted and twisted as the number of layers was restacked. As a result, this restacking technique yields customizable separation performance [143]. Alternative solutions to COF membrane blending production are based on directly growing into the surface of support since the polymeric matrix mixture inhibits the pore surface potential of COFs for membrane separation. Using this technique, Caro and his colleagues created a continuous, high-quality COF membrane supported by industrial ceramic tubes [133b]. A layer of the aldehyde building block must first be functionalized with an amino group before reacting to generate an imine bond. The tube modification was employed to remove dye from the water. It is possible to use this technique to create continuous COF bilayers on a flat, porous alumina substrate [144]. After the functional modification of the substrate, the first synthesis of COF-LZU1 was carried out, then the amino group unreacted on the surface of the COF acted as supported for ACOF1 formation. The interlaced pore of COF-LZU1-ACOF1 membrane performed a great gas separation process due to its appropriate size range. In contrast to MMMs, free-standing COF membranes can also be prepared by processing them without any support or polymeric matrix. The important key to achieving a COF membrane is related to its mechanical properties.

Fig. 14. Schematic representation of COF membrane formation. Adapted from reference 41 with permission of the copyright holders.

An outstanding example was reported by Banerjee and col., in which they used the terracotta process method. COF membranes were prepared (Fig. 14) using PTSA as a catalytic agent, forming a dough, which was processed into a membrane using knife casting before baking [52].

The byproduct water has to be evaporated for the baking process to create the porous ordered framework structure. With a terracotta-like procedure, many types of β -ketamine-connected COF membranes may be created, and these membranes exhibit notable mechanical qualities, such as flexibility.

Jiang and col. recently devised a solution-processing technique that allows for the fabrication of large-area COF membranes by subjecting an amorphous polymeric membrane to a monomer exchange process under solvothermal conditions [145]. The disorder-to-order transformation mechanism was fascinating due to the control over COF membrane thickness and ease of fabrication.

Taking advantage of their low density, high crystallinity, porosity, and excellent mechanical properties of the COF aerogels [49b], they can be compressed into free-standing membranes using optimal compression pressure. The resulting COF membranes exhibited good crystallinity and 50–60 μm thickness, thinner than COF powder counterparts due to the lower density of COF aerogels [81]. Zamora and col. evaluated the permanent porosity of COF membranes by conducting N_2 gas adsorption experiments, which confirmed that the membranes retained their porosity despite some loss due to densification. COF membranes exhibited good gas uptake and selectivity, with higher CO_2 permeability and separation performance than commercial materials. The long-term stability of the COF membranes with moisture was evaluated and showed a relatively steady separation performance for over 120 h. The study provides valuable insights into the potential of COF membranes for gas separation applications. This straightforward compression method for fabricating centimeter-scale imine-based COF-membranes can also be used to obtain COF electrode by incorporating Carbon Super P. Thus, Zamora and col. studied their performance as electrochemical double-layer capacitors, and examined the influence of ion size provided by different electrolytes of these promising COF-electrodes (ECOFs) working with other electrolytes: aqueous (H_2SO_4 1 mol L^{-1}, KOH 6 mol L^{-1}) and an organic electrolyte (tetrabutyl-ammonium hexafluorophosphate ($TBAPF_6$ 0.25 mol L^{-1} in acetonitrile (ACN)). These ECOFs devices perform ideal double-layer charge storage at 100 mV s^{-1} and achieve higher values of areal capacitance for aqueous electrolytes (11.2, and 8.96 mF cm^{-2}). Postulating that ECOFs could become a considerable candidate material for EDLC devices by simply compression [146].

2.8. Potential applications

As previously indicated, bulk COFs are typically created as insoluble

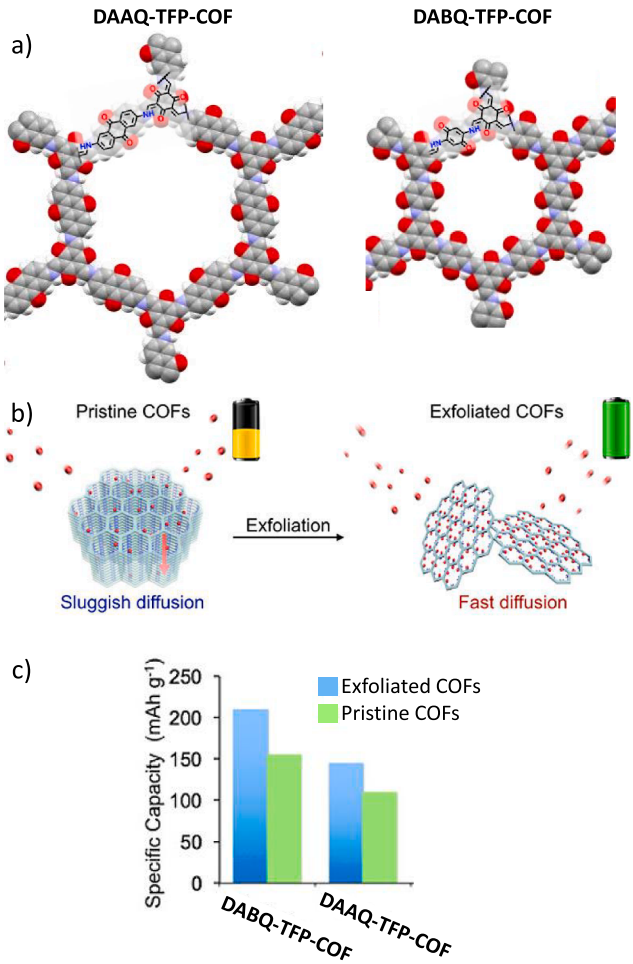

Fig. 15. A) the DAAQ-TFP-COF and DABQ-TFP-COF chemical structures. b) illustration of a schematic for the exfoliation of 2d redox-active COFS into exfoliated cofs for lithium-ion battery cathodes. c) the precise capacity of the DABQ-TFP-COF and DAAQ-TFP-COF batteries after exfoliation and purification. adapted from reference 109a with permission of the copyright holders.

powder solids, which reduces their performance because they are challenging to produce. Demonstrating good and diversified qualities does not enable a competitive performance or durability compared to commercial materials, even though unique processability methods help expand their prospective applications. Few examples of COFs have been demonstrated in actual devices or applications since the processing method's novelty prevents them from performing to their full potential. Developing novel synthetic approaches and investigating fundamental mechanisms and processing effects are crucial to fabricate devices.

However, some of the most impressive examples presented below demonstrate the broad range of possible applications of COFs in some of the most pressing issues the world is currently facing, including energy scarcity, molecular separation, gas separation, and water purification. For instance, COF thin films are a good contender for energy storage applications because of their large surface areas, extremely thin thicknesses, and functional sites. In that regard, Wang and col. created an anthraquinone-based COF (DAAQ-TFP-COF) cathode for lithium-ion batteries (Fig. 15a) [122a].

Delamination via mechanical milling created nanosheets with lower diameters and around a 5 nm thickness, substantially reducing the ion transport channel. According to the electrochemical investigations, its kinetics are regulated by charge transfer, and the redox process occurs at the surface.

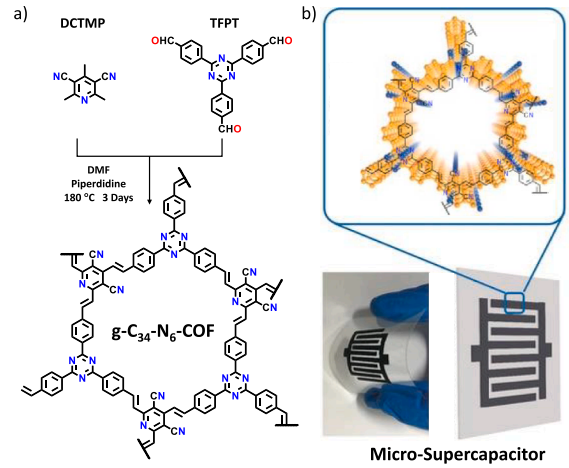

Fig. 16. A) synthesis and structure of g-$C_{34}N_6$-COF and b) Interdigital electrode. Adapted from reference 125 with permission of the copyright holders.

The active sites of the bulk COF with many layers, whose kinetic is controlled by Li-ion diffusion, were not fully used. Therefore, the exfoliation strategy enhances (Fig. 15b) COF performance in the battery showing a specific capacity of 210 mA h g^{-1} with an outstanding 98 % capacity retention at 20 mA g^{-1} and even under fast charge – discharge cycles (500 mA g^{-1}) with a 74 % retention. Zhang and col. provided another intriguing example relating to electrical energy storage.

On a single-walled carbon nanotube, a Knoevenagel condensation was used to create an olefin-linked COF (Fig. 16a) with a distinctive nanofibrous morphology and a fully conjugated network (SWCNTs). The hybrid material was vacuum-filtered using a polytetrafluoroethylene (PTFE) membrane filter to manufacture flexible thin film electrodes [147]. To obtain good electrical conductivity, the planar and completely conjugated triazine core added to the framework provided an unbroken (π-electron delocalization over 2D direction. Furthermore, SWCNTs and nanofibrous shape assembly produced a thin film with exceptional mechanical strength and flexibility. A microsupercapacitor was created utilizing a vacuum-filtrated technique using an interdigitated electrode (MSC) because of the success of obtaining the flexible thin film. The COF-based MSC offered areal capacitances of up to 15.2 mF cm^{-2}, high energy densities of up to 7.3 mWh cm^{-3}, and remarkable rate capability, among the highest values of reported MSCs (Fig. 16b).

Recent studies have shown that COFs play a vital role in regulating the microenvironment of the three-phase interface in high-performance fuel cells [148]. This discovery has significant implications for advancing the practical application of fuel cells and improving their efficiency. Lowering platinum (Pt) loadings without sacrificing power density and durability in fuel cells is a highly desired yet challenging objective due to the high mass transport resistance near the catalyst surfaces. By incorporating ionic CONs into Nafion, the researchers tailored the three-phase microenvironment. This optimization strategy involved optimizing the mesoporous apertures, which measured 2.8 to 4.1 nm, and incorporating appendant sulfonate groups to facilitate proton transfer and promote oxygen permeation. Importantly, the mass activity of Pt and the peak power density of the fuel cell, utilizing Pt/Vulcan (0.07 mg cm^{-2} of Pt in the cathode) in conjunction with the COF, both experienced a remarkable increase of 1.6 times compared to values without COF integration. This effective approach was applied to catalyst layers with different Pt loadings and commercial catalysts. These findings underscore the significance of COFs in regulating the microenvironment of the three-phase interface and offer promising prospects for enhancing fuel cell performance and practical implementation.

Moving on to the molecular separation procedure, industrial protocols must consider sustainability, energy consumption, cost-

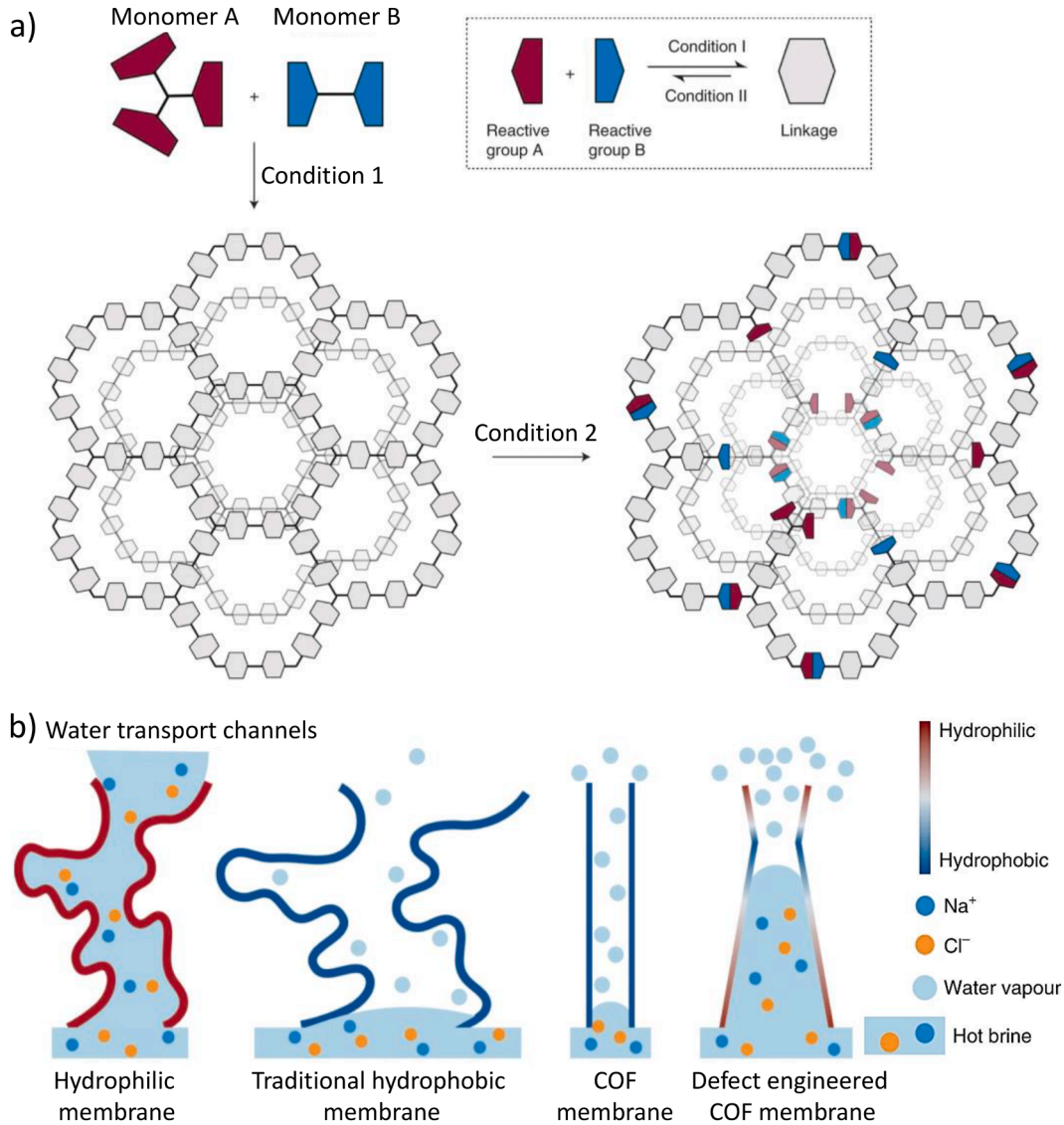

Fig. 17. A) a gradient in cof engineering functionality brought about by competitive reversible covalent bonding. b) during md processes, comparison of various water transport channels in conventional hydrophilic and hydrophobic membranes, a perfect cof membrane, and a cof membrane with a defect. adapted from reference 126 with permission of the copyright holders.

effectiveness, and efficiency. When researchers can fully utilize COF thin films or membranes' pore surface engineering, they will have many applications. A hydrophilicity gradient effect was introduced into the pore matrix within the mesoporous nanochannel, according to a significant example described by Wang and col., ensuring improved water purification performance during desalination [149]. Various times have been used to treat the thin film with an alkaline solution. As time passes, the imine linkage breaks into amine and aldehyde starting monomers, increasing the defects (Fig. 17a). The gradient flaws produce a hydrophilic gradient from the surface to the interior core, which improves the wettability (Fig. 17b). The thin film's thickness and surface are not harmed in the process. The purification operation resulted in a high-water flux of 220 L $m^{-2}h^{-1}$ with *ca.* 100 % NaCl rejection at 0.16 bar. In addition, the thin film demonstrated excellent efficacy against noxious substances like sodium dodecyl sulfate (SDS).

Another intriguing area of research that needs in-depth examinations of framework stability and toxicity is biocompatible COFs. However, the COFs' large surface, long-range order, and network periodicity make it possible to accomplish enormous loads and straightforward transfer of medicinal substances. The potential use of COFs as drug carriers with high loading efficiency and minimal toxicity have been demonstrated by recent investigations. As a tumor-targeted delivery system for anticancer medicines, employing COFs for cancer in vivo is particularly appealing. However, only in vitro study is used to evaluate COFs. In this regard, Jia and col. created PEG-CCM@APTES-COF-1, which combined a polyethylene-glycol-modified curcumin derivative (PEG-CCM) with an amine-functionalized COF to create water-dispersible COF nanocomposites (APTES-COF-1) [150]. PEG-CCM significantly improved the COF nanocomposites' biocompatibility, and the blood circulation time was prolonged. The biodegradation of APTES-COF-1 was started after exposure to the acidic environment prevalent in tumors, and drug delivery was released. The most robust tumor growth inhibition was observed for in vivo anticancer trials compared to other drug delivery agents.

3. Conclusions

In this review, it has been shown that research in COFs has suffered a significant change since their first report in 2005. During the first years, it focused on developing new COF networks and linkage types to expand

the family of materials and better understand their behavior. One of the main issues identified was the lack of chemical stability of the reversible bonds, especially in boron-based COFs, which drove the development of numerous linkages and the addition of functional groups to improve their chemical resistance. These results paved the way for introducing functional moieties in COFs via several strategies resulting in the synthesis of COFs with a wide range of properties that benefit either from their intrinsic porosity or highly ordered structure. Finally, the last challenge that has been identified is the difficulty of integrating COFs in working devices, which has prompted the previous trend of research in the field: methods to process COFs with defined shapes, sizes, and controlled interfaces with other materials. In conjunction with the previous advances in chemistry and functionalization, the formation of oriented thin films over large areas or the successful implementation of additive manufacturing to COFs will bring its use in commercial applications significantly closer.

Declaration of Competing Interest

The authors declare that they have no known competing financial interests or personal relationships that could have appeared to influence the work reported in this paper.

Data availability

No data was used for the research described in the article.

Acknowledgments

This work has been supported by the Spanish MICINN (PID2019-106268GB-C32, and TED2021-129886B-C42) and through the "María de Maeztu" Programme for Units of Excellence in R&D (CEX2018-000805-M). We also thank financial support to the Comunidad de Madrid (MAD2D-CM) and MICINN (Planes complementarios, Materiales Avanzados).

References

[1] P. B. Cyril, Smith, G. E., *Ancient Egyptian medicine : the Papyrus Ebers*, 3rd ed., 1974.
[2] C.W. Scheele, Chemical observations and experiments on air and fire, J. Johnson (1780.).
[3] P.A. Wright, J.A. Connor, Microporous Framework Solids, Royal Soc. Chem. (2007).
[4] H. S. C. Deville, *Reproduction de la Lévyne*, 1862.
[5] L.V.C. Rees, Biogr. Mem. Fellows R. Soc. 44 (1998) 37–49.
[6] S.S. Kistler, Nature 127 (1931), 741.
[7] R. Robson, B.F. Abrahams, S.R. Batten, R.W. Gable, B.F. Hoskins, J. Liu, Supramol. Architect., Am. Chem. Soc. (1992) 256–273.
[8] M. Munakata, T. Kuroda-Sowa, M. Maekawa, A. Honda, S. Kitagawa, Dalton Trans. (1994) 2771–2775.
[9] H. Li, M. Eddaoudi, M. O'Keeffe, O.M. Yaghi, Nature 402 (1999) 276–279.
[10] M. Fujita, J. Yazaki, K. Ogura, J. Am. Chem. Soc. 112 (1990) 5645–5647.
[11] N.B. McKeown, P.M. Budd, Chem. Soc. Rev. 35 (2006) 675–683.
[12] T. Tozawa, J.T.A. Jones, S.I. Swamy, S. Jiang, D.J. Adams, S. Shakespeare, R. Clowes, D. Bradshaw, T. Hasell, S.Y. Chong, C. Tang, S. Thompson, J. Parker, A. Trewin, J. Bacsa, A.M.Z. Slawin, A. Steiner, A.I. Cooper, Nat. Mater. 8 (2009) 973–978.
[13] C.S. Diercks, O.M. Yaghi, Science 355 (2017) eaal1585.
[14] A.P. Cote, A.I. Benin, N.W. Ockwig, M. O'Keeffe, A.J. Matzger, O.M. Yaghi, Science 310 (2005) 1166–1170.
[15] R. Liu, K.T. Tan, Y. Gong, Y. Chen, Z. Li, S. Xie, T. He, Z. Lu, H. Yang, D. Jiang, Chem. Soc. Rev. 50 (2021) 120–242.
[16] K. Geng, T. He, R. Liu, S. Dalapati, K.T. Tan, Z. Li, S. Tao, Y. Gong, Q. Jiang, D. Jiang, Chem. Rev. 120 (2020) 8814–8933.
[17] F. Haase, B.V. Lotsch, Chem. Soc. Rev. 49 (2020) 8469–8500.
[18] H.M. El-Kaderi, J.R. Hunt, J.L. Mendoza-Cortes, A.P. Cote, R.E. Taylor, M. O'Keeffe, O.M. Yaghi, Science 316 (2007) 268–272.
[19] X. Ma, T.F. Scott, Commun. Chem. 1 (2018), 98.
[20] M.J.K. Omar, M. Yaghi, Christian S. Diercks, Introduction to Reticular Chemistry, Wiley - VCH Verlag GmbH & Co. KGaA, 2019, pp. 197–223.
[21] C.R. DeBlase, W.R. Dichtel, Macromolecules 49 (2016) 5297–5305.
[22] L. Xu, X. Zhou, W.Q. Tian, T. Gao, Y.F. Zhang, S. Lei, Z.F. Liu, Angew. Chem., Int. Ed. 53 (2014) 9564–9568.
[23] B.J. Smith, W.R. Dichtel, J. Am. Chem. Soc. 136 (2014) 8783–8789.
[24] P. Kuhn, M. Antonietti, A. Thomas, Angew. Chem., Int. Ed. 47 (2008) 3450–3453.
[25] S. Ren, M.J. Bojdys, R. Dawson, A. Laybourn, Y.Z. Khimyak, D.J. Adams, A. I. Cooper, Adv. Mater. 24 (2012) 2357–2361.
[26] F.J. Uribe-Romo, J.R. Hunt, H. Furukawa, C. Klock, M. O'Keeffe, O.M. Yaghi, J. Am. Chem. Soc. 131 (2009) 4570–4571.
[27] a) Y. Zeng, R. Zou, Z. Luo, H. Zhang, X. Yao, X. Ma, R. Zou, Y. Zhao, J. Am. Chem. Soc. 137 (2015) 1020–1023;
b) X. Chen, M. Addicoat, E. Jin, H. Xu, T. Hayashi, F. Xu, N. Huang, S. Irle, D. Jiang, Sci. Rep. 5 (2015) 14650.
[28] N. Huang, L. Zhai, D.E. Coupry, M.A. Addicoat, K. Okushita, K. Nishimura, T. Heine, D. Jiang, Nat. Commun. 7 (2016) 12325.
[29] Z.-F. Pang, S.-Q. Xu, T.-Y. Zhou, R.-R. Liang, T.-G. Zhan, X. Zhao, J. Am. Chem. Soc. 138 (2016) 4710–4713.
[30] Z. Li, T. Deng, S. Ma, Z. Zhang, G. Wu, J. Wang, Q. Li, H. Xia, S.-W. Yang, X. Liu, J. Am. Chem. Soc. 145 (2023) 8364–8374.
[31] a) H. Lyu, Z. Ji, S. Wuttke, O.M. Yaghi, Chem 6 (2020) 2219–2241;
b) Q. Guan, L.-L. Zhou, W.-Y. Li, Y.-A. Li, Y.-B. Dong, Chem. Eur. J. 26 (2020) 5583–5591.
[32] Y. Huang, X. Hao, S. Ma, R. Wang, Y. Wang, Chemosphere 291 (2022), 132795.
[33] W. Zhang, L. Chen, S. Dai, C. Zhao, C. Ma, L. Wei, M. Zhu, S.Y. Chong, H. Yang, L. Liu, Y. Bai, M. Yu, Y. Xu, X.-W. Zhu, Q. Zhu, S. An, R.S. Sprick, M.A. Little, X. Wu, S. Jiang, Y. Wu, Y.-B. Zhang, H. Tian, W.-H. Zhu, A.I. Cooper, Nature 604 (2022) 72–79.
[34] G. Das, T. Skorjanc, S.K. Sharma, F. Gándara, M. Lusi, D.S. Shankar Rao, S. Vimala, S. Krishna Prasad, J. Raya, D.S. Han, R. Jagannathan, J.-C. Olsen, A. Trabolsi, J. Am. Chem. Soc. 139 (2017) 9558–9565.
[35] S. Altınışık, G. Yanalak, İ. Hatay Patır, S. Koyuncu, ACS Appl. Mater. Interf. 15 (2023) 18836–18844.
[36] J.L. Segura, M.J. Mancheno, F. Zamora, Chem. Soc. Rev. 45 (2016) 5635–5671.
[37] X. Li, Q. Gao, J. Wang, Y. Chen, Z.-H. Chen, H.-S. Xu, W. Tang, K. Leng, G.-H. Ning, J. Wu, Q.-H. Xu, S.Y. Quek, Y. Lu, K.P. Loh, Nat. Commun. 9 (2018), 2335.
[38] J. Maschita, T. Banerjee, G. Savasci, F. Haase, C. Ochsenfeld, B.V. Lotsch, Angew. Chem., Int. Ed. 59 (2020) 15750–15758.
[39] S. Dalapati, S. Jin, J. Gao, Y. Xu, A. Nagai, D. Jiang, J. Am. Chem. Soc. 135 (2013) 17310–17313.
[40] D. Stewart, D. Antypov, M.S. Dyer, M.J. Pitcher, A.P. Katsoulidis, P.A. Chater, F. Blanc, M.J. Rosseinsky, Nat. Commun. 8 (2017), 1102.
[41] A. Nagai, X. Chen, X. Feng, X. Ding, Z. Guo, D. Jiang, Angew. Chem., Int. Ed. 52 (2013) 3770–3774.
[42] a) L. Cusin, H. Peng, A. Ciesielski, P. Samorì, Angew. Chem., Int. Ed. 60 (2021) 14236–14250;
b) E. Vitaku, C.N. Gannett, K.L. Carpenter, L. Shen, H.D. Abruña, W.R. Dichtel, J. Am. Chem. Soc. 142 (2020) 16–20.
[43] P.-F. Wei, M.-Z. Qi, Z.-P. Wang, S.-Y. Ding, W. Yu, Q. Liu, L.-K. Wang, H.-Z. Wang, W.-K. An, W. Wang, J. Am. Chem. Soc. 140 (2018) 4623–4631.
[44] B. Zhang, M. Wei, H. Mao, X. Pei, S.A. Alshmimri, J.A. Reimer, O.M. Yaghi, J. Am. Chem. Soc. 140 (2018) 12715–12719.
[45] A. Acharjya, P. Pachfule, J. Roeser, F.-J. Schmitt, A. Thomas, Angew. Chem., Int. Ed. 58, (2019) 14865–14870.
[46] H. Lyu, C.S. Diercks, C. Zhu, O.M. Yaghi, J. Am. Chem. Soc. 141 (2019) 6848–6852.
[47] A.R. Bagheri, N. Aramesh, J. Mater. Sci. 56 (2021) 1116–1132.
[48] a) W. Zhao, P. Yan, H. Yang, M. Bahri, A.M. James, H. Chen, L. Liu, B. Li, Z. Pang, R. Clowes, N.D. Browning, J.W. Ward, Y. Wu, A.I. Cooper, Nature Synthesis 1 (2022) 87–95;
b) J.A. Martin-Illan, D. Rodriguez-San-Miguel, C. Franco, I. Imaz, D. Maspoch, J. Puigmarti-Luis, F. Zamora, Chem. Commun. 56 (2020) 6704–6707;
c) C. Franco, D. Rodriguez-San-Miguel, A. Sorrenti, S. Sevim, R. Pons, A. E. Platero-Prats, M. Pavlovic, I. Szilagyi, M.L. Ruiz Gonzalez, J.M. Gonzalez-Calbet, D. Bochicchio, L. Pesce, G.M. Pavan, I. Imaz, M. Cano-Sarabia, D. Maspoch, S. Pane, A.J. de Mello, F. Zamora, J. Puigmarti-Luis, J. Am. Chem. Soc. 142 (2020) 3540–3547.
[49] a) D. Zhu, Y. Zhu, Q. Yan, M. Barnes, F. Liu, P. Yu, C.-P. Tseng, N. Tjahjono, P.-C. Huang, M.M. Rahman, E. Egap, P.M. Ajayan, R. Verduzco, Chem. Mater. 33 (2021) 4216–4224;
b) J.A. Martin-Illan, D. Rodriguez-San-Miguel, O. Castillo, G. Beobide, J. Perez-Carvajal, I. Imaz, D. Maspoch, F. Zamora, Angew. Chem., Int. Ed. 60 (2021) 13969–13977.
[50] J. Thote, H. Barike Aiyappa, R. Rahul Kumar, S. Kandambeth, B.P. Biswal, D. Balaji Shinde, N. Chaki Roy, R. Banerjee, IUCrJ 3 (2016) 402–407.
[51] M. Matsumoto, R.R. Dasari, W. Ji, C.H. Feriante, T.C. Parker, S.R. Marder, W. R. Dichtel, J. Am. Chem. Soc. 139 (2017) 4999–5002.
[52] S. Karak, S. Kandambeth, B.P. Biswal, H.S. Sasmal, S. Kumar, P. Pachfule, R. Banerjee, J. Am. Chem. Soc. 139 (2017) 1856–1862.
[53] Y. Zhao, L. Guo, F. Gandara, Y. Ma, Z. Liu, C. Zhu, H. Lyu, C.A. Trickett, E. A. Kapustin, O. Terasaki, O.M. Yaghi, J. Am. Chem. Soc. 139 (2017) 13166–13172.
[54] X. Guan, Y. Ma, H. Li, Y. Yusran, M. Xue, Q. Fang, Y. Yan, V. Valtchev, S. Qiu, J. Am. Chem. Soc. 140 (2018) 4494–4498.
[55] X. Li, Y. Qi, G. Yue, Q. Wu, Y. Li, M. Zhang, X. Guo, X. Li, L. Ma, S. Li, Green Chem. 21 (2019) 649–657.
[56] Z.-B. Zhou, P.-J. Tian, J. Yao, Y. Lu, Q.-Y. Qi, X. Zhao, Nat. Commun. 13 (2022) 2180.
[57] J.L. Segura, S. Royuela, M. Mar Ramos, Chem. Soc. Rev. 48 (2019) 3903–3945.

[58] a) H. Xu, J. Gao, D. Jiang, Nat. Chem. 7 (2015) 905–912;
b) J.A. Martín-Illán, S. Royuela, M. Mar Ramos, J.L. Segura, F. Zamora, Chem. - Eur. J. 26 (2020) 6495–6498.
[59] B. Gui, X. Liu, Y. Cheng, Y. Zhang, P. Chen, M. He, J. Sun, C. Wang, Angew. Chem., Int. Ed. 61 (2022) e202113852.
[60] P.J. Waller, S.J. Lyle, T.M. Osborn Popp, C.S. Diercks, J.A. Reimer, O.M. Yaghi, J. Am. Chem. Soc. 138 (2016) 15519–15522.
[61] F. Haase, E. Troschke, G. Savasci, T. Banerjee, V. Duppel, S. Dörfler, M.M. J. Grundei, A.M. Burow, C. Ochsenfeld, S. Kaskel, B.V. Lotsch, Nat. Commun. 9 (2018), 2600.
[62] J.-M. Seo, H.-J. Noh, H.Y. Jeong, J.-B. Baek, J. Am. Chem. Soc. 141 (2019) 11786–11790.
[63] M.C. Daugherty, E. Vitaku, R.L. Li, A.M. Evans, A.D. Chavez, W.R. Dichtel, Chem. Commun. 55 (2019) 2680–2683.
[64] G. Singh, P.A. Singh, A.K. Sen, K. Singha, S.N. Dubeya, R.N. Handa, J. Choi, Synth. React. Inorg. Met.-Org. Chem. 32 (2002) 171–187.
[65] S.Y. Ding, J. Gao, Q. Wang, Y. Zhang, W.G. Song, C.Y. Su, W. Wang, J. Am. Chem. Soc. 133 (2011) 19816–19822.
[66] J. Guo, D. Jiang, ACS Cent. Sci. 6 (2020) 869–879.
[67] a) T. Ma, E.A. Kapustin, S.X. Yin, L. Liang, Z. Zhou, J. Niu, L.-H. Li, Y. Wang, J. Su, J. Li, X. Wang, W.D. Wang, W. Wang, J. Sun, O.M. Yaghi, Science 361 (2018) 48–52;
b) Y.-B. Zhang, J. Su, H. Furukawa, Y. Yun, F. Gándara, A. Duong, X. Zou, O. M. Yaghi, J. Am. Chem. Soc. 135 (2013) 16336–16339.
[68] J. Dong, Y. Wang, G. Liu, Y. Cheng, D. Zhao, CrystEngComm 19 (2017) 4899–4904.
[69] M. Martínez-Abadía, C.T. Stoppiello, K. Strutynski, B. Lerma-Berlanga, C. Martí-Gastaldo, A. Saeki, M. Melle-Franco, A.N. Khlobystov, A. Mateo-Alonso, J. Am. Chem. Soc. 141 (2019) 14403–14410.
[70] C. Gropp, T. Ma, N. Hanikel, O.M. Yaghi, Science 370 (2020) eabd6406.
[71] J. Li, C. Lin, T. Ma, J. Sun, Nat. Commun. 13 (2022), 4016.
[72] R. Giordano, R.M.F. Leal, G.P. Bourenkov, S. McSweeney, A.N. Popov, Acta Crystallogr. 68 (2012) 649–658.
[73] A.M. Evans, M.R. Ryder, W. Ji, M.J. Strauss, A.R. Corcos, E. Vitaku, N.C. Flanders, R.P. Bisbey, W.R. Dichtel, Faraday Discuss. 225 (2021) 226–240.
[74] X. Chen, M. Addicoat, E. Jin, L. Zhai, H. Xu, N. Huang, Z. Guo, L. Liu, S. Irle, D. Jiang, J. Am. Chem. Soc. 137 (2015) 3241–3247.
[75] S. Kandambeth, D.B. Shinde, M.K. Panda, B. Lukose, T. Heine, R. Banerjee, Angew. Chem., Int. Ed. 52 (2013) 13052–13056.
[76] A.P. Côté, H.M. El-Kaderi, H. Furukawa, J.R. Hunt, O.M. Yaghi, J. Am. Chem. Soc. 129 (2007) 12914–12915.
[77] Z. Mu, Y. Zhu, B. Li, A. Dong, B. Wang, X. Feng, J. Am. Chem. Soc. 144 (2022) 5145–5154.
[78] a) C.H. Feriante, S. Jhulki, A.M. Evans, R.R. Dasari, K. Slicker, W.R. Dichtel, S. R. Marder, Adv. Mater. 32 (2020) 1905776;
b) T. Sick, J.M. Rotter, S. Reuter, S. Kandambeth, N.N. Bach, M. Doblinger, J. Merz, T. Clark, T.B. Marder, T. Bein, D.D. Medina, J. Am. Chem. Soc. 141 (2019) 12570–1912581.
[79] a) L. Yang, H. Yang, H. Wu, L. Zhang, H. Ma, Y. Liu, Y. Wu, Y. Ren, X. Wu, Z. Jiang, J. Mater. Chem. A 9 (2021) 12636–12643;
b) B. Hosseini Monjezi, K. Kutonova, M. Tsotsalas, S. Henke, A. Knebel, Angew. Chem., Int. Ed. 60 (2021) 15153–15164.
[80] N. Huang, R. Krishna, D. Jiang, J. Am. Chem. Soc. 137 (2015) 7079–7082.
[81] J.A. Martin-Illan, J.A. Suarez, J. Gomez-Herrero, P. Ares, D. Gallego-Fuente, Y. Cheng, D. Zhao, D. Maspoch, F. Zamora, Adv. Sci 9 (2022) 2104643.
[82] R.W. Tilford, S.J. Mugavero Iii, P.J. Pellechia, J.J. Lavigne, Adv. Mater. 20 (2008) 2741–2746.
[83] a) Z. Meng, R.M. Stolz, K.A. Mirica, J. Am. Chem. Soc. 141 (2019) 11929–11937;
b) S. Wan, F. Gándara, A. Asano, H. Furukawa, A. Saeki, S.K. Dey, L. Liao, M. W. Ambrogio, Y.Y. Botros, X. Duan, S. Seki, J.F. Stoddart, O.M. Yaghi, Chem. Mater. 23 (2011) 4094–4097;
c) S. Wan, J. Guo, J. Kim, H. Ihee, D. Jiang, Angew. Chem., Int. Ed. 47 (2008) 8826–8830.
[84] G. Bian, J. Yin, J. Zhu, Small 17 (2021) 2006043.
[85] S. Bi, C. Yang, W. Zhang, J. Xu, L. Liu, D. Wu, X. Wang, Y. Han, Q. Liang, F. Zhang, Nat. Commun. 10 (2019), 2467.
[86] a) M. Souto, D.F. Perepichka, J. Mater. Chem. C 9 (2021) 10668–10676;
b) Z. Xie, B. Wang, Z. Yang, X. Yang, X. Yu, G. Xing, Y. Zhang, L. Chen, Angew. Chem., Int. Ed. 58 (2019) 15742–15746.
[87] S. Rager, A.C. Jakowetz, B. Gole, F. Beuerle, D.D. Medina, T. Bein, Chem. Mater. 31 (2019) 2707–2712.
[88] E. Jin, M. Asada, Q. Xu, S. Dalapati, M.A. Addicoat, M.A. Brady, H. Xu, T. Nakamura, T. Heine, Q. Chen, D. Jiang, Science 357 (2017) 673–676.
[89] H. Li, J. Chang, S. Li, X. Guan, D. Li, C. Li, L. Tang, M. Xue, Y. Yan, V. Valtchev, S. Qiu, Q. Fang, J. Am. Chem. Soc. 141 (2019) 13324–13329.
[90] N. Huang, K.H. Lee, Y. Yue, X. Xu, S. Irle, Q. Jiang, D. Jiang, Angew. Chem., Int. Ed. 59 (2020) 16587–16593.
[91] V. Singh, H.R. Byon, Mater. Adv. 2 (2021) 3188–3212.
[92] F. Xu, S. Jin, H. Zhong, D. Wu, X. Yang, X. Chen, H. Wei, R. Fu, D. Jiang, Sci. Rep. 5 (2015) 8225.
[93] Y. Peng, Z. Hu, Y. Gao, D. Yuan, Z. Kang, Y. Qian, N. Yan, D. Zhao, ChemSusChem 8 (2015) 3208–3212.
[94] L. Stegbauer, K. Schwinghammer, B.V. Lotsch, Chem. Sci. 5 (2014) 2789–2793.
[95] H. Wang, H. Wang, Z. Wang, L. Tang, G. Zeng, P. Xu, M. Chen, T. Xiong, C. Zhou, X. Li, D. Huang, Y. Zhu, Z. Wang, J. Tang, Chem. Soc. Rev. 49 (2020) 4135–4165.
[96] N. Huang, X. Ding, J. Kim, H. Ihee, D. Jiang, Angew. Chem., Int. Ed. 54 (2015) 8704–8707.
[97] W.K. Haug, E.M. Moscarello, E.R. Wolfson, P.L. McGrier, Chem. Soc. Rev. 49 (2020) 839–864.
[98] J. Zhao, J. Ren, G. Zhang, Z. Zhao, S. Liu, W. Zhang, L. Chen, Chem. – A Eur. J. 27 (2021) 10781–10797.
[99] S. Jin, X. Ding, X. Feng, M. Supur, K. Furukawa, S. Takahashi, M. Addicoat, M. E. El-Khouly, T. Nakamura, S. Irle, S. Fukuzumi, A. Nagai, D. Jiang, Angew. Chem., Int. Ed. 52 (2013) 2017–2021.
[100] D. Rodriguez-San-Miguel, F. Zamora, Chem. Soc. Rev. 48 (2019) 4375–4386.
[101] S. Kandambeth, K. Dey, R. Banerjee, J. Am. Chem. Soc. 141 (2019) 1807–1822.
[102] S. Karak, K. Dey, A. Torris, A. Halder, S. Bera, F. Kanheerampockil, R. Banerjee, J. Am. Chem. Soc. 141 (2019) 7572–7581.
[103] A.K. Mohammed, S. Usgaonkar, F. Kanheerampockil, S. Karak, A. Halder, M. Tharkar, M. Addicoat, T.G. Ajithkumar, R. Banerjee, J. Am. Chem. Soc. 142 (2020) 8252–8261.
[104] C. Li, J. Yang, P. Pachfule, S. Li, M.Y. Ye, J. Schmidt, A. Thomas, Nat. Commun. 11 (2020), 4712.
[105] F. Li, L.-G. Ding, B.-J. Yao, N. Huang, J.-T. Li, Q.-J. Fu, Y.-B. Dong, J. Mater. Chem. A 6 (2018) 11140–11146.
[106] M. Zhang, L. Li, Q. Lin, M. Tang, Y. Wu, C. Ke, J. Am. Chem. Soc. 141 (2019) 5154–5158.
[107] D. Rodriguez-San-Miguel, A. Abrishamkar, J.A. Navarro, R. Rodriguez-Trujillo, D. B. Amabilino, R. Mas-Balleste, F. Zamora, J. Puigmarti-Luis, Chem. Commun. 52 (2016) 9212–9215.
[108] D.A. Vazquez-Molina, G.S. Mohammad-Pour, C. Lee, M.W. Logan, X. Duan, J. K. Harper, F.J. Uribe-Romo, J. Am. Chem. Soc. 138 (2016) 9767–9770.
[109] C.R. DeBlase, K.E. Silberstein, T.T. Truong, H.D. Abruna, W.R. Dichtel, J. Am. Chem. Soc. 135 (2013) 16821–16824.
[110] J.W. Colson, A.R. Woll, A. Mukherjee, M.P. Levendorf, E.L. Spitler, V.B. Shields, M.G. Spencer, J. Park, W.R. Dichtel, Science 332 (2011) 228–231.
[111] D.D. Medina, J.M. Rotter, Y. Hu, M. Dogru, V. Werner, F. Auras, J.T. Markiewicz, P. Knochel, T. Bein, J. Am. Chem. Soc. 137 (2015) 1016–1019.
[112] R.P. Bisbey, C.R. DeBlase, B.J. Smith, W.R. Dichtel, J. Am. Chem. Soc. 138 (2016) 11433–11436.
[113] N.A.A. Zwaneveld, R. Pawlak, M. Abel, D. Catalin, D. Gigmes, D. Bertin, L. Porte, J. Am. Chem. Soc. 130 (2008) 6678–6679.
[114] K. Dey, M. Pal, K.C. Rout, H.S. Kunjattu, A. Das, R. Mukherjee, U.K. Kharul, R. Banerjee, J. Am. Chem. Soc. 139 (2017) 13083–13091.
[115] Q. Hao, C. Zhao, B. Sun, C. Lu, J. Liu, M. Liu, L.-J. Wan, D. Wang, J. Am. Chem. Soc. 140 (2018) 12152–12158.
[116] M. Matsumoto, L. Valentino, G.M. Stiehl, H.B. Balch, A.R. Corcos, F. Wang, D. C. Ralph, B.J. Mariñas, W.R. Dichtel, Chem 4 (2018) 308–317.
[117] R. Mas-Balleste, C. Gomez-Navarro, J. Gomez-Herrero, F. Zamora, Nanoscale 3 (2011) 20–30.
[118] C. Gibaja, M. Assebban, I. Torres, M. Fickert, R. Sanchis-Gual, I. Brotons, W. S. Paz, J.J. Palacios, E.G. Michel, G. Abellán, F. Zamora, J. Mater. Chem. A 7 (2019) 22475–22486.
[119] D. Hanlon, C. Backes, E. Doherty, C.S. Cucinotta, N.C. Berner, C. Boland, K. Lee, A. Harvey, P. Lynch, Z. Gholamvand, S. Zhang, K. Wang, G. Moynihan, A. Pokle, Q.M. Ramasse, N. McEvoy, W.J. Blau, J. Wang, G. Abellan, F. Hauke, A. Hirsch, S. Sanvito, D.D. O'Regan, G.S. Duesberg, V. Nicolosi, J.N. Coleman, Nat. Commun. 6 (2015), 8563.
[120] I. Berlanga, M.L. Ruiz-González, J.M. González-Calbet, J.L.G. Fierro, R. Mas-Balleté, F. Zamora, Small 7 (2011) 1207–1211.
[121] K.S. Novoselov, D. Jiang, F. Schedin, T.J. Booth, V.V. Khotkevich, S.V. Morozov, A.K. Geim, Proc. Nat. Acad. Sci. 102 (2005) 10451–10453.
[122] a) S. Wang, Q. Wang, P. Shao, Y. Han, X. Gao, L. Ma, S. Yuan, X. Ma, J. Zhou, X. Feng, B. Wang, J. Am. Chem. Soc. 139 (2017) 4258–4261;
b) S. Chandra, S. Kandambeth, B.P. Biswal, B. Lukose, S.M. Kunjir, M. Chaudhary, R. Babarao, T. Heine, R. Banerjee, J. Am. Chem. Soc. 135 (2013) 17853–17861.
[123] a) N. Zhang, T. Wang, X. Wu, C. Jiang, F. Chen, W. Bai, R. Bai, RSC Adv. 8 (2018) 3803–3808;
b) S. Mitra, H.S. Sasmal, T. Kundu, S. Kandambeth, K. Illath, D. Díaz Díaz, R. Banerjee, J. Am. Chem. Soc. 139 (2017) 4513–4520;
c) M.A. Khayum, S. Kandambeth, S. Mitra, S.B. Nair, A. Das, S.S. Nagane, R. Mukherjee, R. Banerjee, Angew. Chem., Int. Ed. 55 (2016) 15604–15608;
d) S. Mitra, S. Kandambeth, B.P. Biswal, A. Khayum, M.C.K. Choudhury, M. Mehta, G. Kaur, S. Banerjee, A. Prabhune, S. Verma, S. Roy, U.K. Kharul, R. Banerjee, J. Am. Chem. Soc. 138 (2016) 2823–2828.
[124] D.W. Burke, C. Sun, I. Castano, N.C. Flanders, A.M. Evans, E. Vitaku, D. C. McLeod, R.H. Lambeth, L.X. Chen, N.C. Gianneschi, W.R. Dichtel, Angew. Chem., Int. Ed. 132 (2020) 5203–5209.
[125] a) H.S. Sasmal, A. Kumar Mahato, P. Majumder, R. Banerjee, J. Am. Chem. Soc. 144 (2022) 11482–11498;
b) S. Karak, K. Dey, R. Banerjee, Adv. Mater. n/a (2022) 2202751.
[126] W. Ma, Q. Zheng, Y. He, G. Li, W. Guo, Z. Lin, L. Zhang, J. Am. Chem. Soc. 141 (2019) 18271–18277.
[127] L. Garzón-Tovar, C. Avci-Camur, D. Rodríguez-San-Miguel, I. Imaz, F. Zamora, D. Maspoch, Chem. Commun. 53 (2017) 11372–11375.
[128] Y.-Y. Liu, X.-C. Li, S. Wang, T. Cheng, H. Yang, C. Liu, Y. Gong, W.-Y. Lai, W. Huang, Nat. Commun. 11 (2020), 5561.
[129] P. Pachfule, S. Kandmabeth, A. Mallick, R. Banerjee, Chem. Commun. 51 (2015) 11717–11720.

[130] D. Rodriguez-San-Miguel, C. Montoro, F. Zamora, Chem. Soc. Rev. 49 (2020) 2291–2302.
[131] G. Li, K. Zhang, T. Tsuru, ACS Appl. Mater. Interfaces 9 (2017) 8433–8436.
[132] C. Zhang, B.-H. Wu, M.-Q. Ma, Z. Wang, Z.-K. Xu, Chem. Soc. Rev. 48 (2019) 3811–3841.
[133] a) D. Hao, J. Zhang, H. Lu, W. Leng, R. Ge, X. Dai, Y. Gao, Chem. Commun. 50 (2014) 1462–1464;
b) H. Fan, J. Gu, H. Meng, A. Knebel, J. Caro, Angew. Chem., Int. Ed. 57 (2018) 4083–4087.
[134] A.M. Evans, I. Castano, A. Brumberg, L.R. Parent, A.R. Corcos, R.L. Li, N. C. Flanders, D.J. Gosztola, N.C. Gianneschi, R.D. Schaller, W.R. Dichtel, J. Am. Chem. Soc. 141 (2019) 19728–19735.
[135] P. Albacete, A. López-Moreno, S. Mena-Hernando, A.E. Platero-Prats, E.M. Pérez, F. Zamora, Chem. Commun. 55 (2019) 1382–1385.
[136] S. Huang, D. Chen, C. Meng, S. Wang, S. Ren, D. Han, M. Xiao, L. Sun, Y. Meng, Small 15 (2019) 1904830.
[137] L. Wang, Y. Xie, Y. Yang, H. Liang, L. Wang, Y. Song, ACS Appl. Nano Mater. 3 (2020) 1412–1419.
[138] L.-L. Wang, C.-X. Yang, X.-P. Yan, ChemPlusChem 82 (2017) 933–938.
[139] a) D. Sun, S. Jang, S.-J. Yim, L. Ye, D.-P. Kim, Adv. Funct. Mater. 28 (2018) 1707110;
b) Y. Peng, M. Zhao, B. Chen, Z. Zhang, Y. Huang, F. Dai, Z. Lai, X. Cui, C. Tan, H. Zhang, Adv. Mater. 30 (2018) 1705454.
[140] Z. Kang, H. Guo, L. Fan, G. Yang, Y. Feng, D. Sun, S. Mintova, Chem. Soc. Rev. 50 (2021) 1913–1944.
[141] B.P. Biswal, H.D. Chaudhari, R. Banerjee, U.K. Kharul, Chem. - Eur. J. 22 (2016) 4695–4699.
[142] Z. Kang, Y. Peng, Y. Qian, D. Yuan, M.A. Addicoat, T. Heine, Z. Hu, L. Tee, Z. Guo, D. Zhao, Chem. Mater. 28 (2016) 1277–1285.
[143] Y. Ying, D. Liu, J. Ma, M. Tong, W. Zhang, H. Huang, Q. Yang, C. Zhong, J. Mater. Chem. A 4 (2016) 13444–13449.
[144] H. Fan, A. Mundstock, A. Feldhoff, A. Knebel, J. Gu, H. Meng, J. Caro, J. Am. Chem. Soc. 140 (2018) 10094–10098.
[145] C. Fan, H. Wu, J. Guan, X. You, C. Yang, X. Wang, L. Cao, B. Shi, Q. Peng, Y. Kong, Y. Wu, N.A. Khan, Z. Jiang, Angew. Chem., Int. Ed. 60 (2021) 18051–18058.
[146] J.Á. Martín-Illán, L. Sierra, P. Ocón, F. Zamora, Angew. Chem. Internat. Ed. 61 (2022) e202213106.
[147] J. Xu, Y. He, S. Bi, M. Wang, P. Yang, D. Wu, J. Wang, F. Zhang, Angew. Chem., Int. Ed. 58 (2019) 12065–12069.
[148] Q. Zhang, S. Dong, P. Shao, Y. Zhu, Z. Mu, D. Sheng, T. Zhang, X. Jiang, R. Shao, Z. Ren, J. Xie, X. Feng, B. Wang, Science 378 (2022) 181–186.
[149] S. Zhao, C. Jiang, J. Fan, S. Hong, P. Mei, R. Yao, Y. Liu, S. Zhang, H. Li, H. Zhang, C. Sun, Z. Guo, P. Shao, Y. Zhu, J. Zhang, L. Guo, Y. Ma, J. Zhang, X. Feng, F. Wang, H. Wu, B. Wang, Nat. Mater. 20 (2021) 1551–1558.
[150] G. Zhang, X. Li, Q. Liao, Y. Liu, K. Xi, W. Huang, X. Jia, Nat. Commun. 9 (2018), 2785.